Relationships between greenhouse gas production and landscape position during short-term permafrost thaw under anaerobic conditions in the Lena Delta

Mélissa Laurent[1], Matthias Fuchs[1], Tanja Herbst[1], Alexandra Runge[1], Susanne Liebner[2,3], Claire C. Treat[1]

[1]Alfred Wegener Institute Helmholtz Centre for Polar and Marine Research, Potsdam, Germany
[2] GFZ German Research Centre for Geosciences, Section Geomicrobiology, Potsdam, Germany
[3] University of Potsdam, Institute for Biochemistry and Biology, Potsdam, Germany

Correspondence to: Mélissa Laurent (melissa.laurent@awi.de)

Abstract. Soils in the permafrost region have acted as carbon sinks for thousands of years. ~~However, as~~As a result of global warming, permafrost soils are thawing and will potentially release ~~more~~ greenhouse gases (GHGs) such as methane (CH_4) and carbon dioxide (CO_2). ~~To address the large~~However, small scale spatial heterogeneities of GHG ~~releases, this study focused on the relationship between CO_2 and CH_4 emissions and soil parameters, as well as the evolution of microbial abundance during a~~production have been neglected in previous incubation studies. Here, we simulated permafrost thaw ~~experiment representing the extent of an Arctic summer~~during growing season~~. Two depths from three Lena Delta cores taken~~ (60 days) along a transect from upland to floodplain ~~were incubated anoxically for 68 days~~ in Kurungnakh Island and then continued the incubation for one year. Potential CO_2 and CH_4 production were measured during an anaerobic incubation experiment using active and permafrost layers from Yedoma and floodplain cores at ~~two different temperatures (4°C~~ and 20~~°C) and an~~°C. An assessment of ~~microbiological~~methanogen abundance ~~(CH_4 producers and aerobic CH_4 oxidizers)~~ was performed in parallel~~. Samples from~~ for the first 60 days. Yedoma samples located in upland or slope position remained in a lag phase during the ~~whole incubation~~growing season simulation, while those ~~from~~ located in the floodplain showed high production of CH_4 (6.5x10^3 µgCH_4-C.gC^{-1}) and CO_2 (6.9x10^3 µgCO_2-C.gC^{-1}~~). Periodic flooding likely allowed the establishment of favorable methanogenic conditions.~~) at 20°C. The ~~presence of higher copy numbers of methanogenic archaea in the active layer of the floodplain than in the upland and slope from the beginning (1.5 to 9.6 times higher) until the end of the incubation time (11 to 700 times higher) supported this hypothesis. In addition, our study pointed out different anaerobic CO_2 production (methanogenesis and other respiration) pathways according to~~permafrost layers of the Yedoma samples started producing CH_4 after six months incubation. We conclude that landscape position is a key factor to trigger CH_4 production during the growing season time in Kurungnakh Island.

Summary. ~~Increasing~~ Climate change is causing increasing temperatures ~~due to climate change cause~~ and permafrost thaw ~~and potentially increasing~~, which might lead to increases in the release of ~~the~~ greenhouse gases CO_2 and CH_4. In this study we investigated the impact of different parameters (temperature, landscape position, and microbes) on the production of these gases during a ~~short-term~~one-year permafrost thaw experiment. For very similar carbon and nitrogen contents, our results show a strong heterogeneity in CH_4 and CO_2 production, as well as in microbial abundance. According to our study, these differences are mainly due to the landscape position and the hydrological conditions established as a result of the topography.

1 Introduction

~~For the past decades, scientists have warned about the effects of global climate change (IPCC 2021). The effects of this warming will be particularly pronounced in the polar regions where the air temperature increase in the past fifty years is already three time higher than the increase in global average during the same period (AMAP, 2021). This particularly affects soils in northern high latitude regions, which contain 1300 Pg of organic carbon (C) (Hugelius et al., 2014). A majority of this C (822~~

Style Definition: List Paragraph
Formatted: Width: 21 cm, Height: 29,7 cm
Formatted: Font: Bold
Formatted: Not Superscript/Subscript
Formatted: Not Superscript/Subscript
Formatted: Not Superscript/Subscript
Formatted: Not Superscript/Subscript
Formatted: Font: Bold
Formatted: Font: +Body (Times New Roman)
Formatted: Font: +Body (Times New Roman)
Formatted: Font: +Body (Times New Roman)
Formatted: Font: +Body (Times New Roman)
Formatted: Font: +Body (Times New Roman)
Formatted: Font: 9 pt

Pg) is stored in permafrost soils (Hugelius et al., 2014), which cover 22% of the Northern Hemisphere (Obu et al., 2019) and store about 352 Pg of organic C within the first meter. Permafrost is defined as ground where the temperature remains at or below 0 °C for more than two consecutive years (Washburn, 1973). Due to low temperatures the organic matter (OM) stored in permafrost soils is characterized by low degradation rate and permafrost soils exist as a C sink (Hugelius et al., 2014). However, during summer, the upper part of the permafrost thaws (active layer) and allows OM decomposition (Lee et al., 2012).

With climate change, warmer soils and permafrost thaw will likely increase and lead to higher OM decomposition rates due to higher microbial activity. Releases of mineralized C into the atmosphere could reduce the permafrost C pool (Dutta et al., 2006; Schuur et al., 2009) and lead to the transformation of Arctic soils from C sinks to C sources which will further increase climate forcing (Koven et al., 2011; Dean et al., 2018; Lara et al., 2019).

The quality and quantity of OM influence GHG emissions by providing decomposable C (Fox and Cleve, 1983; Hobbie, 2000; Kuhry et al., 2020). The C is mineralized and released as carbon dioxide (CO_2) and methane (CH_4) (Wagner et al., 2007; Schuur et al., 2015; Knoblauch et al., 2018).

To quantify CH_4 and CO_2 emissions and to understand C production from thawing permafrost, numerous incubation studies have been carried out (Lee et al., 2012; Knoblauch et al., 2018; Walz et al., 2018; Holm et al., 2020). They found that CH_4 is mainly produced under anoxic conditions; it can also be produced under aerobic conditions, but in much lower quantities (Schuur et al., 2015; Angle et al., 2017). CO_2 is produced under both anaerobic and aerobic conditions. Even though the global warming potential of CH_4 is 34 times higher than that of CO_2 on a 100 year timescale (Wigley, 1998; Myhre et al., 2013; Neubauer and Megonigal, 2015), under oxic conditions CO_2 is released in higher quantity and was considered to contribute more strongly to the permafrost C feedback than CH_4 (Schädel et al., 2016). This understanding has, however, changed recently, with one study showing similar production of CO_2 C equivalents under anaerobic and aerobic conditions (Knoblauch et al., 2018). Therefore, C decomposition under anoxic conditions is a major concern. Indeed, warmer temperatures in permafrost affected soils might lead to wetter soils caused by meltwater from thawing permafrost, and thus to the establishment of anoxic conditions. Nevertheless, it has been shown that not all soils were able to produce the same quantity of CH_4 under anoxic conditions, and some were not able to produce CH_4 even after several years, e.g., they remained in a lag phase (Treat et al., 2015; Knoblauch et al., 2018). Even though a few factors controlling C decomposition have been identified such as organic C quantity, temperature, and oxygen availability in soil (Lee et al., 2012; Schädel et al., 2014; Treat et al., 2015; Knoblauch et al., 2018; Ganzert et al., 2007), earlier incubation studies focused mainly on a single temperature and how C production varies with depth (Lee et al., 2012; Knoblauch et al., 2018; Walz et al., 2018; Holm et al., 2020). Therefore, how different temperatures or landscape positions affect C production under anoxic conditions is not well understood.

Different geochemical and environmental characteristics influence the form and amount of greenhouse gas (GHG) release from permafrost dominated soils. Temperature (Fox and Cleve, 1983; Neff and Hooper, 2002), wetness conditions, and water table position influence the establishment of anoxic conditions (Morrissey and Livingston, 1992; Whiting and Chanton, 1993). In addition, vegetation stimulates GHG release by providing both a transport pathway from the soil to the atmosphere and a nutrients supply in the form of root exudates, such as glucose, to the microbes which play a key role in the C cycle (King and Reeburgh, 2002a).

Furthermore, the topographic position of field sites was shown to be correlated to C emissions (Treat et al., 2018; Elder et al., 2020). However, as shown by high spatial heterogeneities in C emissions across Arctic landscapes (tundra, wetland, thermokarst, lake) (Virtanen and Ek, 2014; Treat et al., 2018; Elder et al., 2020), it is still uncertain what controls C emissions on a local level (Treat et al., 2018; Lara et al., 2019). Areas such as drained tundra have the capacity to offset C emissions by acting as C sinks (Juncher Jørgensen et al., 2015; Treat et al., 2018). However, large CH_4 emissions have been measured in low lying wetlands, like floodplains (Bruhwiler et al., 2014; Oblogov et al., 2020). The identification of C hotspots and C sinks throughout Arctic landscapes is necessary to estimate current and future regional C fluxes and to improve our knowledge of

~~the impact of climate change on permafrost-affected soils. However, until now, although such impacts have been identified, they have been little studied in the context of climate change. Previous studies have mainly sought to elucidate the quantity of C emissions released from different landscape forms (Lee et al., 2012; Schädel et al., 2016; Walz et al., 2018), but few studies have correlated observed heterogeneities in C emissions to landscape position (Treat et al., 2018; Elder et al., 2020).~~

~~Besides soil parameters, several studies identified microbial communities as main controls on C emissions instead of the redox conditions established by environmental settings (Liebner and Wagner, 2007; Wagner et al., 2007; Mackelprang et al., 2011) Mackelprang . In particular, methanogenic archaea, which produce CH_4, and methanotrophic bacteria, which consume CH_4 (Roslev and King, 1996) King, have been detected and identified as crucial for C control in permafrost affected soils (Wagner et al., 2007; Koch et al., 2009; Knoblauch et al., 2018) Koch, Knoblauch, et Wagner 2009. However, it is still not clear whether microbes or redox conditions exert greater control over C emissions. We started a permafrost soil warming experiment using samples from different landscape positions and incubated the samples at two different temperatures in order to elucidate the effect of different temperatures, landscape positions, and microbial communities on C production.~~

~~The aim of this study is to understand and quantify how much C is lost during short-term permafrost thaw~~For the past decades, scientists have warned about the effects of global climate change (IPCC 2021). The effects of this warming will be pronounced in the polar regions where the air temperature increase in the past fifty years is already three times higher than the increase in global average during the same period (AMAP, 2021; Rantanen et al., 2022). This particularly affects soils in northern high latitude permafrost regions, which cover 14,6% of the Northern Hemisphere (Obu et al., 2019) and contain 1300 Pg of organic carbon (C) (Hugelius et al., 2014a). A majority of this C (822 Pg) is stored in permafrost (Hugelius et al., 2014b), which is defined as ground where the temperature remains at or below 0 °C for more than two consecutive years (Washburn, 1973). Due to low temperatures, the organic matter (OM) stored in permafrost soils is characterized by low decomposition rate (Davidson and Janssens, 2006). However, during summer, the upper part of the permafrost affected soils thaws (active layer) and allows OM decomposition (Lee et al., 2012). With climate change, permafrost thaw will likely increase and lead to higher OM decomposition rates, releasing greenhouse gases (GHGs), like carbon dioxide (CO_2), and methane (CH_4; Wagner et al., 2007; Schuur et al., 2015; Knoblauch et al., 2018).This turnover might lead to the transformation of Arctic soils from C sinks to C sources (Koven et al., 2011; Dean et al., 2018; Lara et al., 2019a).

C emissions, and mainly CH_4 emissions greatly differ across Arctic, and especially within small scales (Treat et al., 2018; Lara et al., 2019a; Elder et al., 2020) . Treat et al., (2018) showed in their study that flux variability was strongly associated to specific geomorphology components of the landscape which affects factors like soil moisture and site drainage (e.g., landscape position). Landscape position is highly affected by permafrost thaw, low-lying ice-reach permafrost areas can turn out water-logged environments following permafrost thaw, while higher areas can be drained by water run-off. The water-logged areas like thermokarst, lakes, or wetlands have been identified as CH_4 emissions hotspots (Olefeldt et al., 2013; Treat et al., 2018; Kuhn et al., 2021) because of the anaerobic conditions that favour methanogen communities (Conrad, 2002; Yavitt et al., 2006). On the other hand, well-drained sites such as upland tundra, have the capacity to offset CH_4 emissions by acting as CH_4 sinks due to net oxidation in the surface soil (Juncher Jørgensen et al., 2015; Treat et al., 2018). Hence, after permafrost thaw, the redox conditions, established by the landscape position, lead to different microbial communities and ultimately CH_4 emissions (McCalley et al., 2014).

To quantify CH_4 and CO_2 production and to understand C turnover from thawing permafrost, numerous incubation studies have been carried out (Lee et al., 2012; Knoblauch et al., 2018; Walz et al., 2018; Holm et al., 2020). Studies have shown that C decomposition was depending on several factors such as organic C quantity, OM quality, temperature, and oxygen availability in soil (Ganzert et al., 2007; Lee et al., 2012; Schädel et al., 2014; Treat et al., 2015; Knoblauch et al., 2018). Additionally, Treat et al., (2015) highlighted that CH_4 production differences were partly explained by the landscape position. For incubation under aerobic conditions, Kuhry et al., (2020) demonstrated that landscape categories gave a good estimation of SOM lability, and therefore explained better CO_2 production than %C only. Unlike incubation under aerobic conditions

(Kuhry et al., 2020), few studies have specifically focused on how the landscape position affects CO_2 and CH_4 production, and whether landscape position is a good indicator for estimating CO_2 and CH_4 production (Treat et al., 2018; Elder et al., 2020). Besides landscape position, climate change affects the environmental factors in the study region, it modifies weather conditions and plays a key role in controlling rain events (frequency and intensity) (Callaghan et al., 2010; Tabari, 2020; Wang et al., 2021; Fewster et al., 2022). During the past 60 years the precipitation in Siberia has increased by 2.6mm/decade over the year Wang et al., (2021). This finding leads likely to wetter condition during the growing season in Siberia, and therefore, soil moisture increase. Changes in soil moisture will impact vegetation cover, soil redox conditions. Increase of precipitations will also lead to deepen active layer (Zhu et al., 2017; Douglas et al., 2020), hence, release bioavailable C from the upper part of the permafrost layers. Waldrop et al., (2010) identified more labile C to CO_2 production in shallow permafrost than in the active layer. On the other hand, other incubation experiments showed higher C turnover into CO_2 in the active layer (Walz et al., 2017; Faucherre et al., 2018). Regarding CH_4 production, studies tend to show higher CH_4 production in the active layer than shallow permafrost (Treat et al., 2015), but some studies also measured the opposite behaviour among their samples (Wagner et al., 2007; Waldrop et al., 2010). Therefore, it is still unclear how much CO_2 and CH_4 can be produced from shallow permafrost. Furthermore, high CH_4 production heterogeneities, as well as long lag time have been measured with samples from Kurungnakh Island (Knoblauch et al., 2013, 2018). Hence, the question whether the methanogen communities will have the time to activate during the growing season under anaerobic condition remains.

The aim of this study is to simulate permafrost thaw under wet growing season conditions across different landscape units ~~at our model study area~~ in the Lena Delta, Siberia~~. This study measures GHG emissions based on an incubation experiment~~ and ~~focuses on~~measure CO_2 and CH_4 production. Here, we incubated upland Yedoma and adjacent lowland floodplain samples under anaerobic conditions, and focused on the relationships between GHG ~~emissions~~production and microbial abundance shifts ~~during~~following short-term (growing season length) and longer-term (1 year) permafrost thaw~~ under anaerobic conditions~~. The objectives of the study were to: (1) quantify CH_4 and CO_2 production ~~during a short term~~over one year under anaerobic incubation; (2) establish relationships between CH_4 and CO_2 production and ~~microbes (methanogens and methanotrophs);~~methanogen abundances; and (3) ~~identify settings and controls that drive~~characterize the role of the landscape position on gas production ~~rates~~ in thawed permafrost soils~~.~~ during a growing – season time (60 days).

Formatted: Font: Not Bold

2 Materials and methods

2.1 Site description and sampling

Soil samples were collected in August 2018 on Kurungnakh Island (72.333 N, 126.283 E), Lena Delta, Siberia (Figure 1~~). Kurungnakh Island is located in the continuous permafrost zone and is an erosional remnant of Late Pleistocene deposits, characterized by ice- and organic-rich sediments (Grigoriev, 1993; Schwamborn et al., 2002) ; most of the island is composed of fluvial sandy sediments and Yedoma Ice Complex (IC) deposits. The IC is made up of ice-saturated sediments (65% to 90%), composed of cryoturbated silty sands and peaty deposits of Holocene origin (Schwamborn et al., 2002; Schirrmeister et al., 2011, 2013). Sediments from the Yedoma IC contain on average 3% total organic carbon (TOC) (Strauss et al., 2013); IC sediments, however, can include organic-rich layers, with TOC content reaching more than 20% in layers with the highest C content. Thermokarst lakes and wetlands are part of Kurungnakh Island due to thermo-erosional activity (Morgenstern et al., 2021). Samples were also collected in the modern Kurungnakh Island floodplain area. Modern floodplains in the Lena River Delta are of Holocene deltaic origin and are composed of stratified middle to fine sands and silts with layers of autochthonous peat and allochtonous OM (Schwamborn et al., 2002; Boike et al., 2013). The soil sampling was carried out in two stages: first, the active layer was extracted using a spade and active layer samples were collected using a fixed volume cylinder (250 cm^3). Then, after excavating the active layer, permafrost soil cores were sampled to a depth of one meter below surface, by drilling with a modified snow ice and permafrost (SPIRE) auger (Jon Holmgren's Machine Shop, Alaska, USA). For this~~

~~study, three cores were selected due to their location within the local topography: P15, P16, and P17. They were located on an upland, on a slope, and on a floodplain, respectively (Figure 1), with a well-drained upland soil profile. These cores were chosen on the basis of geographical proximity to each other, landscape position, moisture gradient, and ice composition.~~

170). Kurungnakh Island is located in the continuous permafrost zone and is an erosional remnant of Late Pleistocene deposits, characterized by ice- and organic-rich sediments (Grigoriev, 1993; Schwamborn et al., 2002) ; most of the island is composed of fluvial sandy sediments and Yedoma Ice Complex (IC) deposits. The IC is made up of ice-saturated sediments (65% to 90%), composed of cryoturbated silty sands and peaty deposits of Holocene origin (Schwamborn et al., 2002; Schirrmeister et al., 2011, 2013). Sediments from the Yedoma IC contain on average 3% total organic carbon (TOC) (Strauss et al., 2013a), 175 however, IC sediments can include organic-rich layers, with TOC content reaching more than 20% in layers. Kurungnakh Island is characterised by thermokarst lakes and wetlands due to thermo-erosional activity (Morgenstern et al., 2021). Samples were also collected in the young Kurungnakh Island floodplain area. The young and active floodplains in the Lena River Delta are of Holocene deltaic origin and are composed of stratified middle to fine sands and silts with layers of autochthonous peat and allochtonous OM (Schwamborn et al., 2002; Boike et al., 2013).

180 The soil sampling was carried out in two stages. First, the active layer was extracted using a spade and active layer samples were collected using a fixed volume cylinder (250 cm^3). Then, permafrost soil cores were sampled to a depth of one meter below surface, by drilling with a modified snow ice and permafrost (SPIRE) auger (Jon Holmgren's Machine Shop, Alaska, USA). For this study, three cores were selected, two were from the Yedoma deposits (P15 and P16) and one belonged to a floodplain area (P17). They were located on an upland, on a slope, and on a floodplain, respectively (Figure 1), with a well-185 drained upland soil profile (Supplementary Fig 1). The Yedoma upland was sloping towards three directions. For this transect, the slope samples were collected in the north-eastern slope. The floodplain samples were taken in the highest part of the floodplain, 5 m above the Lena River water level.

These cores were chosen on the basis of geographical proximity to each other, landscape position, moisture gradient, and ice composition. The three cores had an organic layer ranging between three and seven cm (Yedoma and floodplain respectively). 190 Below this organic-surface layer, the soil cores were identified as mineral soil. The permafrost layers from the Yedoma cores were ice-rich, while no visible ice structure was seen for the floodplain core (Table 1).

Cores were described and subsampled in the field. Detailed core descriptions are presented in Table 1 and Supplementary Table 1. For the purpose of our study, we chose two samples from each core, one from the active layer and ~~another~~one from the frozen layer (above 1 m depth to simulate shallow permafrost thaw; Supplementary Table 1). Care was taken not to select 195 samples from the top of the active layer in order to avoid the top organic layers. Cores were subsampled in a climate chamber at -4 °C with a hammer and a chisel instead of a saw, to limit contamination.

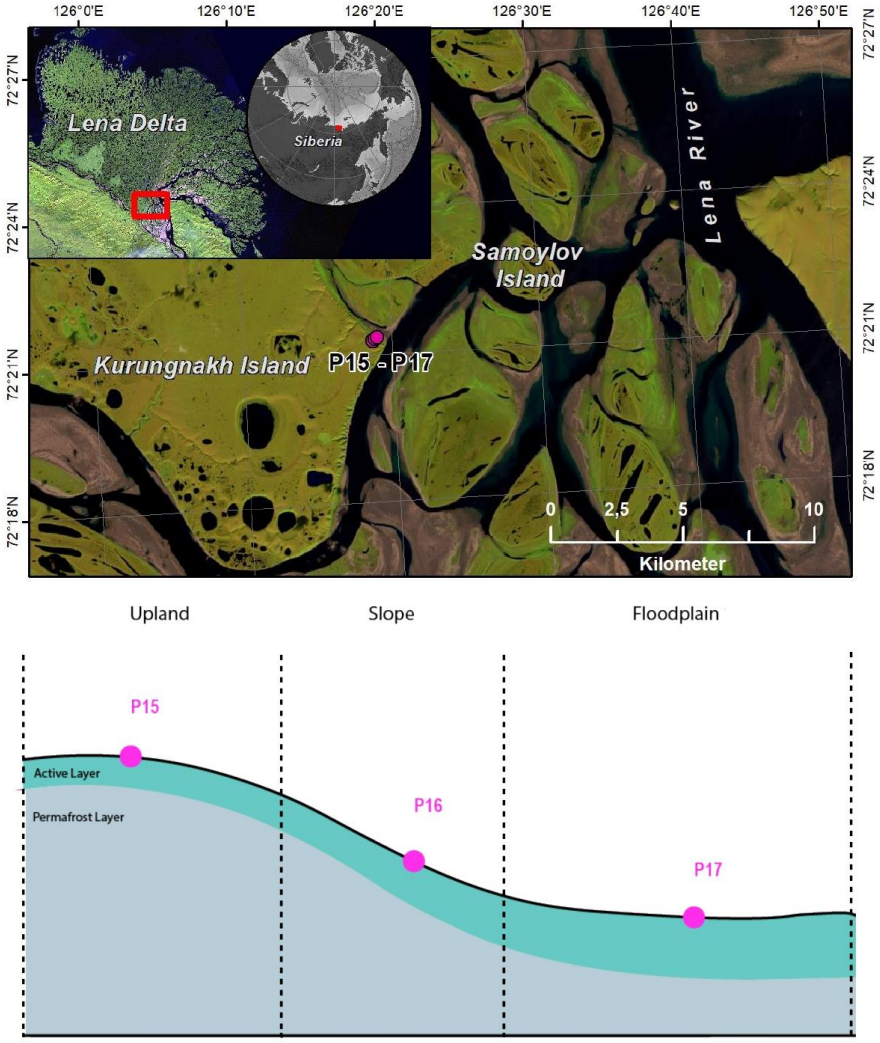

Figure 1: Location of Kurungnakh Island in the Lena Delta (Siberia). The location of the cores used for the study are indicated on the map (a.) and along a schematic transect (b.). Samples were taken during the Lena summer expedition in 2018.

2.2 Sedimentary and geochemical characterization

We characterized the samples for soil texture, C and nitrogen contents, water content, electronic conductivity, and pH. First, samples were thawed at 4° C overnight; then the pore water was extracted with a rhizon soil moisture sampler ~~(Meijboom and van Noordwijk, 1991). Electrical conductivity and pH were measured from pore water for better comparison between samples. Prior to further analyses, soil samples were freeze-dried and the absolute water content (wet weight – dry weight divided by wet weight) was calculated. For TOC, Total Carbon (TC), and Total Nitrogen (TN), subsamples were homogenized and measured with a carbon-nitrogen-sulfur (CNS) analyzer (Elementar Vario EL III). Each subsample was measured in duplicate,~~

and for each series of measurements, standards and blanks were used to ensure reliable analytical measurements. In order to calculate C and N storage for each sample, bulk density was determined based on a relationship between absolute water content and bulk density (Fuchs et al., 2018) (Meijboom and van Noordwijk, 1991). Electrical conductivity and pH were measured from pore water. Prior to further analyses, soil samples were freeze-dried and the absolute water content (Eq 1) was calculated. For TOC weight percent, Total Carbon (TC), and Total Nitrogen (TN), subsamples were homogenized and measured with a carbon-nitrogen-sulfur (CNS) analyzer (Elementar Vario EL III). Each subsample was measured in duplicate, and, standards and blanks were used to ensure reliable analytical measurements. The bulk density was determined based on a transfer function between absolute water content and bulk density made by Fuchs, (2019) (Supplementary Fig 2). Since most of the samples used to establish this correlation came from the same area as our samples, we assumed that the transfer function was applicable to our samples. Another subsample was used for grain size characterization. The grain size analysis was conducted using a laser diffraction particle size analyzer (Mastersizer 3000). Prior to measuring, subsamples were put on a heated shaker for three weeks and H_2O_2 was added daily to remove the organics. The samples were measured in a wet dispersion unit and at least three subsamples from each sample were measured. In the end, the average grain size distribution (in vol%) was calculated from the measured replicates.

Carbon storages were calculated by multiplying the TOC contents with the bulk density and then divided by the sample length. Another subsample was used for grain size characterization. The grain size analysis was conducted using a laser diffraction particle size analyzer (Mastersizer 3000). Prior to measuring, subsamples were put on a heated shaker for three weeks and H_2O_2 was added daily to remove the organic materials. The samples were measured in a wet dispersion unit and at least three subsamples from each sample were measured. The average grain size distribution (in vol%) was calculated from the measured replicates.

$$\Theta = \frac{W_w - W_d}{W_w} \quad \text{Eq(1)}$$

Where Θ is for water content, W_w is wet weight, and W_d dry weight.

2.3 Incubation set-up and substrate addition

The To mimic a wet growing season the samples were first incubated under anaerobic conditions for 60 days at two different temperatures, 4 °C and 20 °C. Since most of the samples did not produce CH_4 after two months incubation, we extended the incubation time to 363 days to see whether the other cores would produce CH_4. For every sample, three replicates were incubated resulting in a total of 36 samples. Prior to incubation, the samples were thawed at 4°C and prepared under oxygen-free conditions using an anoxic glovebox. The samples were homogenized and 13g of wet soil was collected and inserted into a 120 mL vial. We added sterilizedSterilized tap water was added only to samples with a moisture content of less than 30% to limit the effect of gas dissolution (Henry's Law). The amount of Sterilized tap water was calculated to reach 30% moisture, based on the original water content and the weight (wet and dry). The flasks were closed with rubber stoppers and aluminium lids. The headspace of the samples was flushed with pure nitrogen for three minutes to remove potential O_2 inside the vials. The samples were incubated in the dark.

After 60 days of incubation, 0.7 mg glucose per gram dry sample weight were added to two of the three replicates to understand the effect of potential substrate limitation in the soil system. The glucose was diluted with milli-Q water to obtain a 100 $g.L^{-1}$ solution. Solutions were injected via syringe to minimize soil disturbance (Pegoraro et al., 2019).(Pegoraro et al., 2019). The same amount of water as was added within the glucose solution was added to the third replicate to ensure that differences in gas production were only due to the addition of glucose (Pegoraro et al., 2019; Adamczyk et al., 2021). The glucose addition was also carried out under oxygen-free conditions.

The effects of glucose are usually observed very quickly, which means within less than 48h (Yavitt et al., 1997; Pegoraro et al., 2019)(Yavitt et al., 1997; Pegoraro et al., 2019). Therefore, after the glucose addition, gas was measured daily for one

Field Code Changed

week. (described in the following section). As the first injection had little effect on gas production a second injection (day 64) was added with twice the amount of glucose solution (1.4 mg glucose per gram dry sample weight).

2.4 Gas analyses

CO_2 and CH_4 in the headspace were measured with a gas chromatograph (GC) (7890A, Agilent Technologies, USA) with flame ionization detection (FID). The temperature in the column was 50 °C with a flow of 15 mL/min and a runtime of 4.5 minutes. Helium was used as a carrier gas. A Hamilton syringe was used to introduce 250 µL of gas into the GC. For the first week, measurements were made every two days, then twice a week for three weeks, then once a week until day 60. The incubation vials were flushed when either CH_4 or CO_2 concentration reached 1x 10^4 ppm to avoid gas saturation inside the flask. Finally, the production rate was calculated according to the method of Robertson et al. (1999) and normalized per gram soil C. The production rate was calculated with the change in concentration of CO_2 and CH_4 over the incubation time. First the concentration was converted using the ideal gas law and then used a linear regression between each measurement point to calculate the change in concentration over time. Then the mineralisation rate was calculated with the headspace and the volume of the dry content and normalized per gram soil C (Robertson et al., 1999). For samples with pH>7, water contents were very low (Table 1), therefore we assumed that a negligible amount of CO_2 was stored as DIC in the sample water and did not correct the calculation for the pH. However, we are aware that this might underestimate C mineralization.

The impact of glucose on CH_4 and CO_2 production was quantified as a glucose factor, calculated using the cumulative C emissionsproduction at 67 days and referred to a glucose factor.

$$Gf = \frac{(P_{gt} - P_t)}{P_t}$$

Where Gf is glucose factor (%), P_{gt} is total CH_4 production rate for samples with glucose, and P_t is total CH_4 production rate at i days for samples without glucose.

2.5 Quantification of methanotrophic and methanogenic gene copy numbers

Methanotrophic bacteria and methanogenicMethanogenic archaea were quantified with quantitative Polymerase Chain Reaction (qPCR) at different times during the incubations.: when the samples were still frozen (1); after 60 days of incubation (2); and after glucose addition (67 days of incubation) (3). However, due to laboratory restrictions during the Corona virusCovid-19 pandemic, it has onlynot been possible to analyze 26 samples instead of 90. We decided to analyze onlyanalyse all the incubated vials. Only one replicate for eachper sample at three different times: when the samples were still frozen (1); after 60 days of incubation (2); and after glucose addition (3).for the first two runs were analysed. For the last pointrun, we selected the two samples with the highest CH_4 production rates after the glucose addition among the six samples the active layers of P16 and P17. Each sample was replicated three times

Since methanotroph bacteria are good indicators of the oxidation level under in-situ condition, they were quantified with qPCR before starting the incubation.

Key genes coding for the enzyme methyl coenzyme-M reductase (*mcrA*) (Thauer, 1998)(Thauer, 1998) and for the enzyme particulate methane monooxygenase (*pmoA*) (Theisen and Murrell, 2005)(Theisen and Murrell, 2005) were examined to identify methanogens and methanotrophs, respectively. DNA extractions were performed with a GeneMATRIX Soil DNA purification kit according to the manufacturer's protocol. After DNA extraction, the DNA concentration was quantified by fluorescence with the Qubit dsDNA HS Assay Kit (Invitrogn, United States). Gene copy numbers were quantified using a SYBRGreen qPCR assay using the KAPA SYBRFAST qPCR Master Mix (Sigma-Aldrich, Germany) on a CFX96 real-time thermal cycler (Bio-Rad Laboratories Inc., United States). All runs were performed in technical triplicates and each run was completed through melt-curve analysis in order to check for specificity of the assay (Liebner et al., 2015).(Liebner et al., 2015). Methanogenic archaea were targeted with the primer set mlas-F/*mcrA*-R (Hales et al., 1996)(Hales et al., 1996).

To amplify the methanogenic archaea *mcrA* gene, PCR samples were kept at 95 °C for 5 min to denature the DNA. The amplification process was performed with 40 denaturation cycles at 95°C for 1 min, annealing at 60°C for 45 s, and elongating at 72°C for 90 s. To ensure complete amplification, samples were kept at 80°C for 10 min. In addition, to amplify the methanotrophic *pmoA* gene, using primer pmoA189-F and primer pmoAmb661-R two PCR reaction conditions were used. The first PCR comprised initial denaturation at 95°C for 5 min, 30 cycles with denaturation at 94°C for 45 s, decreasing annealing temperature from 64°C to 52 °C for 60 s, elongation at 72°C for 90s, and final elongation at 80°C for 90 s. The second PCR comprised an initial denaturation and polymerase activation at 95 °C for 5 min, 22 cycles of denaturation at 94°C for 45 s, annealing at 56°C for 60 s, elongation at 72°C for 90 s, and a final extension at 72°C for 10 min.

2.6 Statistical analyses

~~We used Q10 to measure the temperature sensitivity of the samples. Q10 shows the proportional change in production rates for an increase of 10 degrees. Q10 was chosen as it is a temperature indicator used in numerous studies, and therefore allows an easier comparison with other studies (Waldrop et al., 2010; Lupascu et al., 2012; Treat et al., 2015). In addition, for small ranges of temperature such as in our study, Q10 is a reliable indicator (Hamdi et al., 2013). Q10 was calculated via the "equal-time" method, meaning that fluxes from the two temperatures were compared after the same incubation time (Hamdi et al., 2013).~~

The gas production and microbial data did not show a normal distribution; consequently, it was not possible to test for differences by performing an ANOVA. The differences between cores and depths, and also the impact of temperature on gas production and microbes, were therefore tested using the ~~Kuskal~~Kruskal-Wallis test with the R function, kruskal.test().

~~All statistics and results analyses were performed with R version 4.0.5 (R Core Team, 2021).~~

All statistics and results analyses were performed with R version 4.0.5 (R Core Team, 2021).

3 Results

3.1 Soil characteristics

All soil samples had a pH between 6.5 -7.5, except P15-F, were in a pH range of 6.5–7.5. Most electrical conductivities were very low (<200 µS.cm^{-1}), except for two samples: P16-F and P17-A (635 µS.cm^{-1}; Table 1).(Table 2). Water content was higher in permafrost (54.5%-60.8%) than in the active layer (23.7%-25.8%) for the two yedoma cores, P15 and P16. In contrast, in P17The water content was higher in the active layer (36.2%) than in the permafrost layer (in the floodplain core P17 (36.2% vs. 17.2%) (Table 1%; Table 2).

Sediment TOC ranged from 0.172% to 3.81%.8%. Most TOC was slightly lower in the active layer of P16 comparedcontents ranged from 2.7% to P15; the opposite was observed for the permafrost layer. Concerning P17, TOC content in the active layer was close to the P15 TOC content. The3.8% but the TOC content in the permafrost layer of P17 was the lowest of the six samples. (0.2%; Table 2). All the samples had TOC below 6%, and therefore they were considered as mineral soils (%C < 12%) (Table 1Table 2) (Soil Survey Staff, 2014)(Soil Survey Staff, 2014).

TN contents were very low for all the samples (>(<0.3%). TN%) and was below the detection limit of the laser analyzer (below 0.1%) for P17-F. C:N ratios wereranged between 12 and 20. The highest ratios were measured in P15; the lowest were in P17P16. The C:N ratio was higher in the permafrost layer of P15 than in the active layer.

There were no differences inThe C stock ranged from 2.3 to 38.8 kg.m^{-3}. The active layers for all the samples were higher than 30 kg.m^{-2} while, the highest C stock in the permafrost layer was 19 kg.m^{-3} in the Yedoma core P16. The permafrost layer of the floodplain had the lowest C storage, more than ten times lower than samples from the active layers (Table 2).

The grain size distribution was similar between P15 and P16. The active layer of P17 contained more clay than and the least sand of the other samples, and P17 was the least sandy sample. In contrast to the active layer, the frozen layer of P17while permafrost in P17-F was the sandiest sample (Table 1).(Supplementary Table 1).

Table 1: ~~Chemical and physical properties of the active and frozen layers of the three samples. The conductivity temperature reference was 25°C. Numbers in brackets are standard deviations.~~**Soil description and vertical position of the sampling cores.**

~~Samples~~	~~Depth (cm)~~	~~Layer~~	~~Landscape position~~ ~~Horizon~~	~~pH~~ ~~Soil description~~	~~Conductivity (µS/cm)~~	~~Dry Bulk density (g cm^{-3})~~	~~Water content (%)~~	~~TOC (%)~~	~~C/N ratio~~	~~Sand (%)~~	~~Silt (%)~~	~~Clay (%)~~
~~P15-A~~	41.5	Active	~~Upland~~ Mineral	~~6.75~~Compacts silt, grey, with brown organic inclusions	~~164.5~~	~~1.12~~	~~25.8~~	~~3.54~~	~~18.13~~	~~31.42~~	~~50.23~~	~~18.22~~
~~P15-F~~	81.5	Permafrost	~~Upland~~Mineral	~~6.06~~Ataxilic ice structure, silt grey	~~150.2~~	~~0.41~~	~~60.8~~	~~2.70~~	~~20.59~~	~~28.75~~	~~53.45~~	~~17.81~~
~~P16-A~~	38.5	Active	~~Slope~~Mineral	~~7.21~~Silt, brown,	~~98.6~~	~~1.18~~	~~23.7~~	~~2.70~~	~~12.95~~	~~30.09~~	~~50.8~~	~~19.13~~

Formatted: Left, Line spacing: single
Inserted Cells
Deleted Cells
Formatted: Font: Italic
Formatted: Font: Italic
Deleted Cells
Deleted Cells
Deleted Cells
Deleted Cells
Formatted: Position: Horizontal: Left, Relative to: Column, Vertical: In line, Relative to: Margin, Horizontal: 0 cm, Wrap Around
Formatted: Justified, Position: Horizontal: Left, Relative to: Column, Vertical: In line, Relative to: Margin, Horizontal: 0 cm, Wrap Around
Deleted Cells
Formatted: Font: 10 pt, Not Bold, Italic, Font color: Auto
Deleted Cells
Deleted Cells
Formatted: Font: 10 pt, Not Bold, Italic, Font color: Auto
Formatted: Font: 10 pt, Not Bold, Italic, Font color: Auto
Formatted: Font: Italic
Formatted: Position: Horizontal: Left, Relative to: Column, Vertical: In line, Relative to: Margin, Horizontal: 0 cm, Wrap Around
Formatted: Font: 10 pt, Not Bold, Italic, Font color: Auto
Formatted: Justified, Position: Horizontal: Left, Relative to: Column, Vertical: In line, Relative to: Margin, Horizontal: 0 cm, Wrap Around
Formatted: Font: 10 pt, Font color: Auto
Formatted: Position: Horizontal: Left, Relative to: Column, Vertical: In line, Relative to: Margin, Horizontal: 0 cm, Wrap Around
Formatted: Justified, Position: Horizontal: Left, Relative to: Column, Vertical: In line, Relative to: Margin, Horizontal: 0 cm, Wrap Around
Formatted: Font: 10 pt, Font color: Auto
Formatted: Font: Italic
Formatted: Position: Horizontal: Left, Relative to: Column, Vertical: In line, Relative to: Margin, Horizontal: 0 cm, Wrap Around
Formatted: Justified, Position: Horizontal: Left, Relative to: Column, Vertical: In line, Relative to: Margin, Horizontal: 0 cm, Wrap Around
Formatted: Position: Horizontal: Left, Relative to: Column, Vertical: In line, Relative to: Margin, Horizontal: 0 cm, Wrap Around
Formatted: Justified, Position: Horizontal: Left, Relative to: Column, Vertical: In line, Relative to: Margin, Horizontal: 0 cm, Wrap Around
Formatted: Font: 10 pt, Font color: Auto
Formatted: Font: Italic
Formatted ...
Formatted ...
Formatted ...
Formatted ...

				organic rich, slightly sandy									
P16-F	102.5	Permafrost	Slope	Mineral	7.06	Silt, grey-brown, structureless to micro-lenticular	479	0.51	54.5	3.81	12.67	26.73	55.12	18.07
P17-A	31.5	Active	Floodplain	Mineral	7.22	Organic rich silt, slighlty sandy	635	0.88	36.2	3.48	18.46	18.89	45.40	35.72
P17-F	78.5	Permafrost	Floodplain	Mineral	7.44	Sand, no visible ice	86.4	1.36	17.2	0.17		96.26	3.1	0.48

Table 2: Summary table of Q10 values, CO_2:CH_4 ratios, and glucose factors. Means of Q10 for CH_4 and CO_2 total emissions after 61 days of incubation. Q10<1 indicates negative effect of temperature on gas production, equal to 1 indicates no effect of temperature on gas production, and Q10>1 indicates positive effect of temperature on gas production. Means of total emission CO_2:CH_4 ratio at 20 °C and 4 °C after 60 days of incubation. Glucose factors were calculated 7 days after glucose addition for each sample with total C emissions. Positive values indicate positive impact of glucose on GHG production and negative values means less CH_4 production after glucose addition.

Samples	***Layer***	***Mean Q10***		***Mean CO_2:CH_4***		***Glucose Factor (%)***			
		CH_4	CO_2	4 °C	20 °C	CH_4 4 °C	CH_4 20 °C	CO_2 4 °C	CO_2 20 °C
P15-A	Active	0.9 ± 0.5	2.4 ± 0.7	1455.9 ± 99.9	5515.7 ± 2731.9	-0.10	-0.38	0.02	0.18
P15-F	Permafrost	2.6 ± 1.2	2.6 ± 1.8	1687.7 ± 590.8	1544.5 ± 402.1	0.02	-0.31	-0.20	-0.44
P16-A	Active	2.7 ± 1.1	6.6 ± 3.4	2157.6 ± 456.5	5168.1 ± 1245.6	-0.41	0.70	-0.02	1.22
P16-F	Permafrost	13.1 ± 22.3	6.0 ± 0.9	246.1 ± 231.7	1710.1 ± 1405.2	0.40	-0.93	0.11	3.23
P17-F	Active	6006.8 ± 2771.9	8.8 ± 3.2	707.3 ± 8.1	1.1 ± 0.1	-0.01	0.24	0.51	0.60
P17-F	Permafrost	21.8 ± 10.4	3.2 ± 1.6	64.2 ± 9.5	12.6 ± 11.9	1.18	0.27	-0.11	0.82

Table 2: Chemical and physical properties of the active and frozen layers of the three cores. The conductivity temperature reference was 25°C. Numbers in brackets are standard deviations

Samples	***pH***	***Conductivity (µS/cm)***	***TOC (%)***	***C/N ratio***	***C (kg.m^{-3})***	***Water content (weight %)***
P15-A	6.75	164.5	3.54	18.13	38.8	25.8
P15-F	6.06	150.2	2.70	20.59	9.4	60.8
P16-A	7.21	98.6	2.70	12.95	35.2	23.7
P16-F	7.06	479	3.81	12.67	18.5	54.5
P17-A	7.22	635	3.48	18.46	30.0	36.2
P17-F	7.44	86.4	17.2		2..3	17,2

Formatted: English (United States)
Formatted: Font: Italic
Formatted: Position: Horizontal: Left, Relative to: Column, Vertical: In line, Relative to: Margin, Horizontal: 0 cm, Wrap Around
Formatted: Justified, Position: Horizontal: Left, Relative to: Column, Vertical: In line, Relative to: Margin, Horizontal: 0 cm, Wrap Around
Formatted: Position: Horizontal: Left, Relative to: Column, Vertical: In line, Relative to: Margin, Horizontal: 0 cm, Wrap Around
Formatted: Justified, Position: Horizontal: Left, Relative to: Column, Vertical: In line, Relative to: Margin, Horizontal: 0 cm, Wrap Around
Formatted: Font: 10 pt, Font color: Auto
Formatted: Font: 10 pt, Font color: Auto
Formatted: Font: Italic
Formatted: Position: Horizontal: Left, Relative to: Column, Vertical: In line, Relative to: Margin, Horizontal: 0 cm, Wrap Around
Formatted: Justified, Position: Horizontal: Left, Relative to: Column, Vertical: In line, Relative to: Margin, Horizontal: 0 cm, Wrap Around
Formatted: Position: Horizontal: Left, Relative to: Column, Vertical: In line, Relative to: Margin, Horizontal: 0 cm, Wrap Around
Formatted: Justified, Position: Horizontal: Left, Relative to: Column, Vertical: In line, Relative to: Margin, Horizontal: 0 cm, Wrap Around
Formatted: English (United States)
Formatted: Font: Italic
Formatted: Position: Horizontal: Left, Relative to: Column, Vertical: In line, Relative to: Margin, Horizontal: 0 cm, Wrap Around
Formatted: Font: 10 pt, Not Bold, Italic, Font color: Auto
Formatted: Justified, Position: Horizontal: Left, Relative to: Column, Vertical: In line, Relative to: Margin, Horizontal: 0 cm, Wrap Around
Formatted: Font: 10 pt, Font color: Auto
Formatted: Font: 10 pt, Font color: Auto
Formatted: Font: 10 pt, Font color: Auto
Formatted: Font: 9 pt

3.2 Potential gas production

3.2.1 ~~Effect of temperature on~~ CH_4 production over one year incubation

~~Gas production was monitored for 60 days (~~At the end of 363-day incubation, nearly all cores and depths produced CH_4 at 20°C incubation (Figure 2~~). At the end of incubation, most samples did not show consistent CH_4 production at both 4 °C and 20 °C (Figure 2a; Figure 2b; Figure 3). CH_4 production rates were always below 0.4 µg CH_4-C .g C^{-1}.d^{-1} and total CH_4 production below 7 µg CH_4-C .gC^{-1}. The active layer of P17 at 20 °C was the only sample that consistently produced CH_4 throughout the incubation. Its lag time ended after 14 days of incubation (Figure 2c) and the maximum CH_4 production rate (355.52 ± 77.16 µg C- CH_4.g C^{-1}.d^{-1}) was reached after 33 days of incubation. Production then stabilized until the end of incubation (Figure 2c). CH_4 production for P17-F-20 started after 47 days of incubation (Figure 2c), for a total amount of 42.53 ± 15.79 µg CH_4 .C .g C^{-1} (Figure 3).~~

~~Significant differences in total CH_4 production between cores were only shown at 20 °C (F= Kruskal-Wallis, df = 1, p = 0.0034). CH_4 production in core P17 was higher in the active layer, at both 4 °C and 20 °C, than in permafrost. CH_4 emissions were larger at 20 °C than at 4 °C for the two depths (F= Kruskal-Wallis, df = 1, p = 0.049). Q_{10} in P17 for the active layer (6006.76 ± 2771.88) and permafrost layer (21.84 ± 10.38) were consistent with these results (Table 2). P15 and P16 behaved similarly, with higher CH_4 production for the active layer at 4 °C than at 20 °C (F= Kruskal-Wallis, df = 1, p = 0.0065 and F= Kruskal-Wallis, df = 1, p = 0.0374, respectively), and no difference for the permafrost layer. CH_4 production was not found to differ between the active layer and permafrost layer at 20 °C for P15 and P16. However, at 4 °C, CH_4 production from P15 was higher in the active layer than in the permafrost layer (F= Kruskal-Wallis, df = 1, p = 0.04953). Even though the total CH_4 production of P15 and P16 showed differences according to the temperature or to the depth, their CH_4 production rates were very low and therefore, regarding CH_4 production, they were still considered in the lag phase after 60 days of incubation.~~

~~3.2.2 Effect of temperature on~~; Figure 3). The floodplain active layer (P17-A) was the sample with the highest cumulative CH_4 production over the time (917,2 ± 150 µg CH_4-C .g DW^{-1}). After 6 months of incubation, the CH_4 production rate of P17-A decreased and then plateaued. The floodplain permafrost core (P17-F) produced 1% of this amount of CH_4 (0.5 ± 0.2 µg CH_4-C .g DW^{-1}) at 20°C. The permafrost layers at 20°C of both Yedoma cores (P15 and P16) produced similar amounts of CH4 (20.5 ± 6.1 µg CH_4-C .g DW^{-1} and 159 ± 104 µg CH_4-C .g DW^{-}1, respectively) while methane production from the active layers of these cores was minimal (P16-A: 3.34 ± 0.25 µg CH_4-C .g DW^{-1}; P15-A: 0.51± 0.14 µg CH_4-C .g DW^{-1}). Cumulative CH_4 production at 4 C was limited to one sample, the active layer of the floodplain core (Figure 2; Figure 3). Cumulative production of the other cores was less than 1 µg CH_4-C g DW^{-1} after 1 year (Figure 2a; Figure 2b; Figure 3).

The lag time before CH_4 production was observed ranged from 14 days to over 363 days. The active layer of the floodplain core (P17-A-20) was the first to produce CH_4 after 14 days of incubation at 20 C. The frozen layers of Yedoma the cores required at least 6 months incubation to start producing CH_4 at 20°C (Figure 2; Table 2) but in the active layer of the Yedoma cores, CH_4 production took substantially longer: 273 days P16-A-20 while P15-A did not produce CH_4 over 363 days in the experiment. At 4 C, CH_4 production in P17-A started after 333 days but was not observed for the other samples (Figure 2; Table 3).

When the CH_4 production were expressed per dry weight, the results showed cumulative production around 30 times lower than the production per gC, but with similar patterns except for the active layer of the Yedoma core P16. With a cumulative CH_4 production reaching 123 µg CH_4-C g C^{-1} this sample was not considered in the lag phase anymore (phase before the beginning of CH_4 production; Supplementary Fig 3).

3.2.2 CO_2 production over one year incubation

~~A decrease of CO_2 production at the beginning of incubation was observed for all the samples (~~Over the 363-day incubation, cumulative CO_2 production ranged from 90,3 µg CO_2-C.g^{-1}DW to 701,4 µg CO_2-C.g^{-1}DW. The cumulative CO_2 production

of P17-A at 20 °C, was the highest among all the samples (701,4 ± 124 µg CO_2-C.g^{-1}DW) and the permafrost layer of the same core at 4°C was the lowest (Figure 2). Overall, temperature had no impact on CO_2 production in the permafrost layers (F= Kruskal-Wallis, df = 1, p = 0.1711) (Table 2, Figure 3b). Concerning the active layers, only P16 and P17 showed a decrease of CO_2 production with decreasing temperature (F= Kruskal-Wallis, df = 1, p = 0.0495) (Table 2-Q10). However, after day 33, CO_2 production started to decrease for P17-A-20 (Figure 2f). For all cores, CO_2 production in the active layer was higher than in the permafrost layer at 4 °C and 20 °C (respectively: F= Kruskal-Wallis, df = 1, p = 0.0152; F= Kruskal-Wallis, df = 1, p = 0.0003) (Figure 3). As with CH_4 production, CO_2 production of P15 and P16 did not differ under different temperatures. Similarly, the cumulative CO_2 release for P17-A, as for CH_4, was the highest among all samples (6887.79 ± 933.27 µg CO_2-C.gC^{-1}) at 20 °C.

The CO_2: CH_4 production ratio of P17 at 4 °C and 20 °C was in each case the lowest indicating methanogenic conditions. ; Figure 3). The CO_2 production of P15 and P16 were in the same range, between 142 ± 85 µg CO_2-C.g^{-1}DW (P16-A at 4deg) and 348,3 ± 135 µg CO_2-C.g^{-1}DW (P15-F at 20°C) (except P16-F at 4°C); (F= Kruskal-Wallis, df = 1, p = 0.20) (Figure 2; Figure 3). The permafrost layers of the Yedoma core P16 at 4d°C and the floodplain had cumulative production below 60 µg CO2-C.g^{-1}DW. The results per gC showed a different pattern for the cumulative CO_2 production of the floodplain core P17. The permafrost layer at 4°C reached 7,98 mg CO_2-C.gC^{-1} and had higher CO_2 production than the permafrost layer at 20°C and the active layer at 4°C. (Supplementary Fig 3)

A decrease of CO_2 production at the beginning of incubation was observed for all the samples (Figure 2). All the active layers samples (except the active layer of the floodplain P17 at 4°C), as well as the permafrost layers of the Yedoma cores P15, P16 at 20 °Creached the maximum production rates of CO_2 before or at the end of the first two months (Figure 2). The maximum production rate of CO_2 for the active layer of the floodplain at 4°Cwas attained after 300-day incubation and the other permafrost samples reached the maximum production rate between 2 and 5 months (Figure 2). Maximum production rates ranged between 16.3 µg C- CO_2.g C^{-1}.d^{-1} (P16-F) and 754 µg C- CO_2.g C^{-1}.d^{-1} (P17-F) at 4°C, and between 77.6 and 284 µg C- CO_2.g C^{-1}.d^{-1} for P16-F and P17-A, respectively at 20°C (Supplementary Table 2). After half a year of incubation, CO_2 production plateaued for all the samples. For all the samples, we noticed an increase of CO_2 production after 60-day incubation, e.g., after the microbial sampling, following by a decrease of the CO_2 production. We did not consider those results to describe the maximum production rates.

After one year of incubation, neither the temperature nor the depth impacted the cumulative CO_2 production of the cores (F= Kruskal-Wallis, df = 1, p = 0.09), Figure 2, Figure 3). CO_2 production was higher at 20 C only for the permafrost layer of the Yedoma core P16 and the active layer of the floodplain P17 (F= Kruskal-Wallis, df = 1, p < 0.05) (Figure 2; Figure 3).

The P17-A-20 CO_2: CH_4 ratio decreased rapidly during the first 14 days, reached one after 40 days and remained stable until the end of incubation (Table 2

Table 3). TheAs well, the CO_2: CH_4 ratio of P17-F-20A at the end4°C and P16-F at 20°C were low after 363 days of incubation reached 12.55 ± 11.93. At 4 °C (respectively, 2.7 ± 2.6 and 2.6 ± 2.1). For all the P17-A samples, except P15-F, CO_2: CH_4 ratio was 700 times higherratios were significantly lower at 20°C than at 20 °C, while for P17-F the ratio was only five times higher4°C (Table 2Table 2).

Formatted: Font: Bold

~~For the other samples, ratios remained high (246.11 ± 231.69 – 5515.66 ± 2731.85) until the end of incubation at both 4 °C and 20 °C (Table 2), which is consistent with the long lag phases and indicates a marginal contribution of CH_4-C.~~

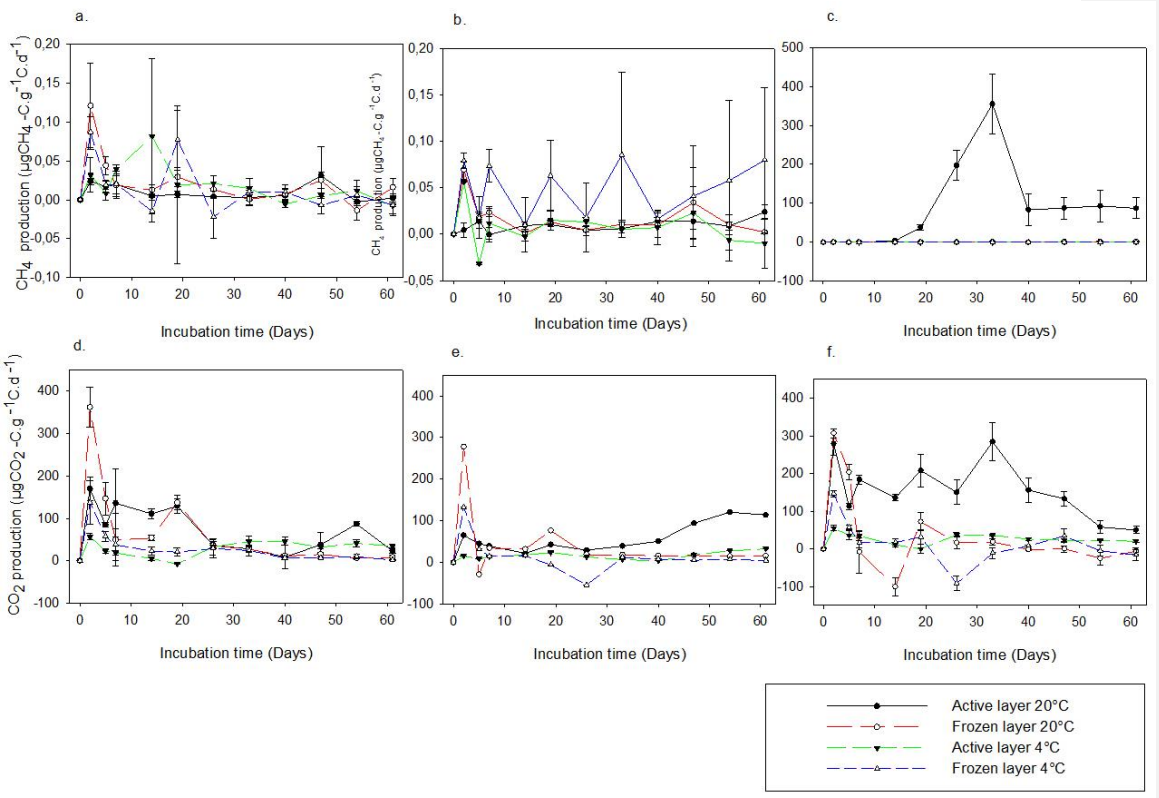

~~Figure 2: Gas production at 4 °C and 20 °C for 60 days of incubation. CH_4 production of (a.) P15, (b.) P16 and (c.) P17. CO_2 production of (d.) P15, (e.) P16 and (f.) P17. Error bars show the deviation from the means ± standard error (n=3). Note differing y-axis scales between cores.~~

~~Figure 3: Cumulative production of CO_2 and CH_4 after 60 days of incubation at 4°C and 20°C. Scale is expressed as square root in order to have a better display.~~

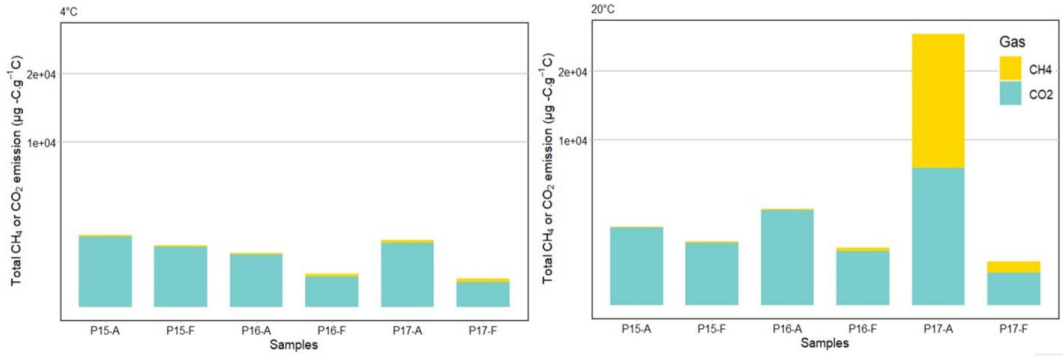

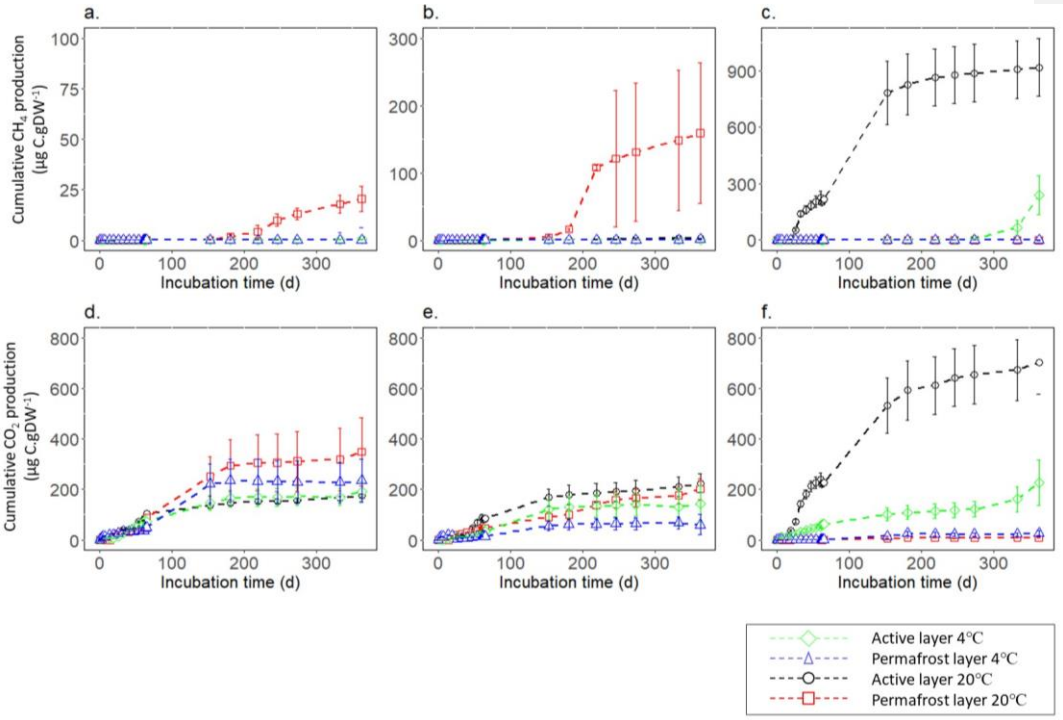

440

Figure 2: Cumulative gas production per gram dry weight (DW) at 4 °C and 20 °C for 363 days of incubation. CH_4 production of (a.) P15, (b.) P16 and (c.) P17. CO_2 production of (d.) P15, (e.) P16 and (f.) P17. Error bars show the standard deviation from the means ± standard error (n=3). Note differing y-axis scales between cores for CH_4

445

Figure 3: Cumulative production per gram dry wet of CO_2 and CH_4 after 60 days of incubation at 4°C and 20°C and after 363 days. AL stands for "Active layer" and PL stands for "Permafrost Layer". Scale is expressed as square root in order to have a better display.

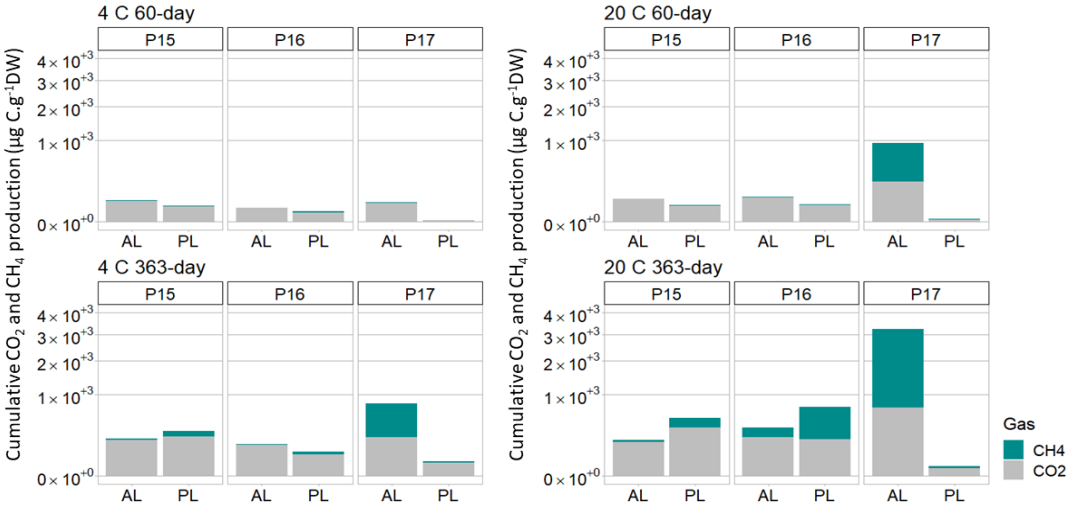

Formatted: Highlight

Table 3: ~~Means of cumulative production of CH_4 and~~Summary table of lag time, CO_2 ~~(per gram C) at 4 °C and 20 °C after 61~~:CH_4 ratios, and glucose factors. Lag time is expressed in days, L.T. stands for samples where the lag time did not end after 1 year incubation. Means of total emission CO_2:CH_4 ratio at 20 °C and 4 °C after 363 days of incubation ~~(n=3).~~

~~Samples~~	~~Layer~~	~~Mean Total CH_4 emissions at 4 °C ($\mu g\ CH_4.C.gC^{-1}$) (n = 3)~~	~~Mean Total CO_2 emissions at 4 °C ($\mu g\ CO_2.C.gC^{-1}$) (n = 3)~~	~~Mean Total CH_4 emissions at 20 °C ($\mu g\ CH_4.C.gC^{-1}$) (n = 3)~~	~~Mean Total CO_2 emissions at 20 °C ($\mu g\ CO_2.C.gC^{-1}$) (n = 3)~~
~~P15-A~~	~~Active~~	~~6.96 ± 1.17~~	~~1803.48 ± 255.36~~	~~0.51 ± 0.27~~	~~2184.38 ± 99.11~~
~~P15-F~~	~~Permafrost~~	~~1.30 ± 0.35~~	~~1332.17 ± 494.62~~	~~0.99 ± 0.32~~	~~1414.07 ± 141.75~~
~~P16-A~~	~~Active~~	~~1.61 ± 0.43~~	~~1012.44 ± 179.93~~	~~0.66 ± 0.13~~	~~3309.28 ± 587.99~~
~~P16-F~~	~~Permafrost~~	~~11.20 ± 8.45~~	~~340.81 ± 30.54~~	~~4.34 ± 5.21~~	~~1074.83 ± 47.79~~
~~P17-A~~	~~Active~~	~~10.55 ± 1.50~~	~~1519.87 ± 1052.87~~	~~6 539.02 ± 1299.21~~	~~6887.79 ± 933.27~~
~~P17-F~~	~~Permafrost~~	~~0.49 ± 0.10~~	~~230.80 ± 8.36~~	~~42.53 ± 15.79~~	~~390.60 ± 140.38~~

~~3.2.3 Effect of glucose addition~~

. **Glucose factors were calculated** 7 days after glucose addition for each sample with total C productions. Positive values indicate positive impact of glucose on GHG production and negative values means less CH_4 production after glucose addition.

Formatted: Font: 9 pt

~~together with total CH_4:CO_2 production rates (Table 2).~~

Samples	*Layer*	*Lag Time (days)*		*Mean CO_2:CH_4*		*Glucose Factor*			
		20C	4C	4 °C	20 °C	CH_4 4 °C	CH_4 20 °C	CO_2 4 °C	CO_2 20 °C
P15-A	Active	L.T.	L.T.	$522.6 \pm 1.7x10^{+2}$	$409.1 \pm 2.2x10^{+2}$	-0.10	-0.38	0.02	0.18
P15-F	Permafrost	153	L.T.	$1930.1 \pm 2.2x10^{+3}$	$2236.8 \pm 3.9x10^{+3}$	0.02	-0.31	-0.20	-0.44
P16-A	Active	274	L.T.	$1661.4 \pm 1.5x10^{+2}$	$50.1 \pm 4.0x10^{+1}$	-0.41	0.70	-0.02	1.22
P16-F	Permafrost	181	L.T.	$195.5 \pm 1.3x10^{+2}$	2.5 ± 2.1	0.40	-0.93	0.11	3.23
P17-A	Active	14	333	2.7 ± 2.7	0.8 ± 0.1	-0.01	0.24	0.51	0.60
P17-F	Permafrost	L.T.	L.T.	$266.9 \pm 1.8x10^{+2}$	$34.8 \pm 4.2x10^{+1}$	1.18	0.27	-0.11	0.82

3.2.3 Effect of glucose addition

Overall, no effect of glucose injection on CH_4 production was detected ~~at the end of the~~ after 67-day incubation ~~period (Table 2(~~

Table 3) (F= Kruskal-Wallis, df = 1, p = 0.5913). ~~However, a~~A production peak was detected one day after the second glucose addition for P15 and P16. ~~Nevertheless, these variations~~The response factors were ~~very~~ low (an increase of 0.8 and 9.1~~%)~~ over the control) and appeared only at 20 °C. ~~The variations may be due to the disturbance of the equilibrium due to the dilution of the gas in the water (Henry's law). P16-F-20 without added glucose showed higher CH_4 production than with added glucose. The reason for this is likely the higher CH_4 production for this replicate, already observed before glucose addition; therefore, the difference in CH_4 production was not correlated to glucose addition.~~ No impact from the glucose addition was detected on CH_4 production for the samples at 4°C after either the first or the second injection (Supplementary ~~Figure 2).~~ Fig 5). While glucose addition increased CO_2 production at 20 °C ~~was higher for samples that received glucose~~ by 46% (~~Table 2~~

Table 3) (F= Kruskal-Wallis, df = 1, p ~~=~~< 0.~~0192~~05), no difference in CO_2 production was detected for any of the samples at 4°C after glucose addition (Supplementary Figure ~~2**Erreur ! Source du renvoi introuvable.**). In addition, CO_2: CH_4 ratios after 67 days of incubation (with and without glucose addition) were compared (data not shown). No differences were seen between samples with and without glucose addition at both temperatures for all the cores.~~5).

3.3 Gene copy numbers of methanogens and methanotrophs

~~We quantified aerobic methanotrophic bacteria and~~ For half of the samples, no methanogenic ~~archaea using qPCR. Methanogenic~~ gene copy numbers ~~based on the *mcrA* gene ranged from $7.6x10^1$ to $5.85x10^3$ copies per gram wet weight~~ were detected when the samples were ~~still frozen (~~thawed prior to beginning the incubation. From these samples, only the methanogenic gene copy number for core P16-F were above the detection limit ($4.3x10^3$). Therefore, it was not possible to compare the methanogenic gene copy numbers before the beginning of the incubation. (Figure 4~~).~~)

After 60 days of incubation, the *mcrA* gene copy numbers ranged from ~~$7.62x10^2$~~$5.35x10^3$ to $5.34x10^5$~~, depending on temperature.~~. The qPCR results showed significant differences between cores ~~when the samples were still frozen (F= Kruskal-Wallis, df = 1, p = 0.0085) as well as~~ after 60 days of incubation (F= Kruskal-Wallis, df = 1, p ~~=~~< 0.~~0025). In both cases, P17-A had~~05) with the highest copy number per gram soil (~~Figure 4~~Figure 4c~~). P15 showed no difference between the active and~~) in P17-A. No methanogenic gene copy numbers were detected for the permafrost layer ~~or between 4 °C and 20 °C after 60 days of incubation.~~ of P17, as well as the active layer of P16.

P16-F and P17-A had 9 times and 36 times higher copies per gram soil, respectively at 20 °C ~~($4.77 x10^4$ and $5.34 x10^5$)~~ than at 4 °C (~~$5.35 x10^3$ and $1.49 x10^4$) (~~F= Kruskal-Wallis, df = 1, p ~~= 0.04953). Gene copy numbers~~ < 0.05) (Figure 4). The temperature response for the active and permafrost layer of P15 was not identified because the results were below detection limit at both, 4°C and 20°C.

Similarly, no comparison was possible between active and permafrost layers for all the samples.

Gene copy numbers of methanotrophic bacteria based on the *pmoA* gene, before the incubation, were either below detection limit, or not detected, therefore no interpretation on the oxic conditions under field condition was possible (Figure 4).

Gene copy numbers after addition of glucose did not differ from those without glucose (~~Figure 4d).~~Figure 4).

~~Gene copy numbers of methanotrophic bacteria based on the *pmoA* gene were mostly between $1x10^2$ and $5 x10^2$ copies per gram soil. No differences were found between P16 and P17 at both 4 °C and 20 °C. Similarly, no difference was found after 60 days. P16-F with glucose had a higher copy number per gram soil than the sample without glucose at both 4°C and 20°C. No difference after the addition of glucose was found for P17-A (Figure 4h). In core P15 *pmoA* could not be detected in any~~

Formatted: Highlight

of the treatments, except for the active layer at 4°C. The absence of detectable concentrations is likely due to an insufficient number of microbes in these samples (low DNA concentration) (Supplementary Table 3).

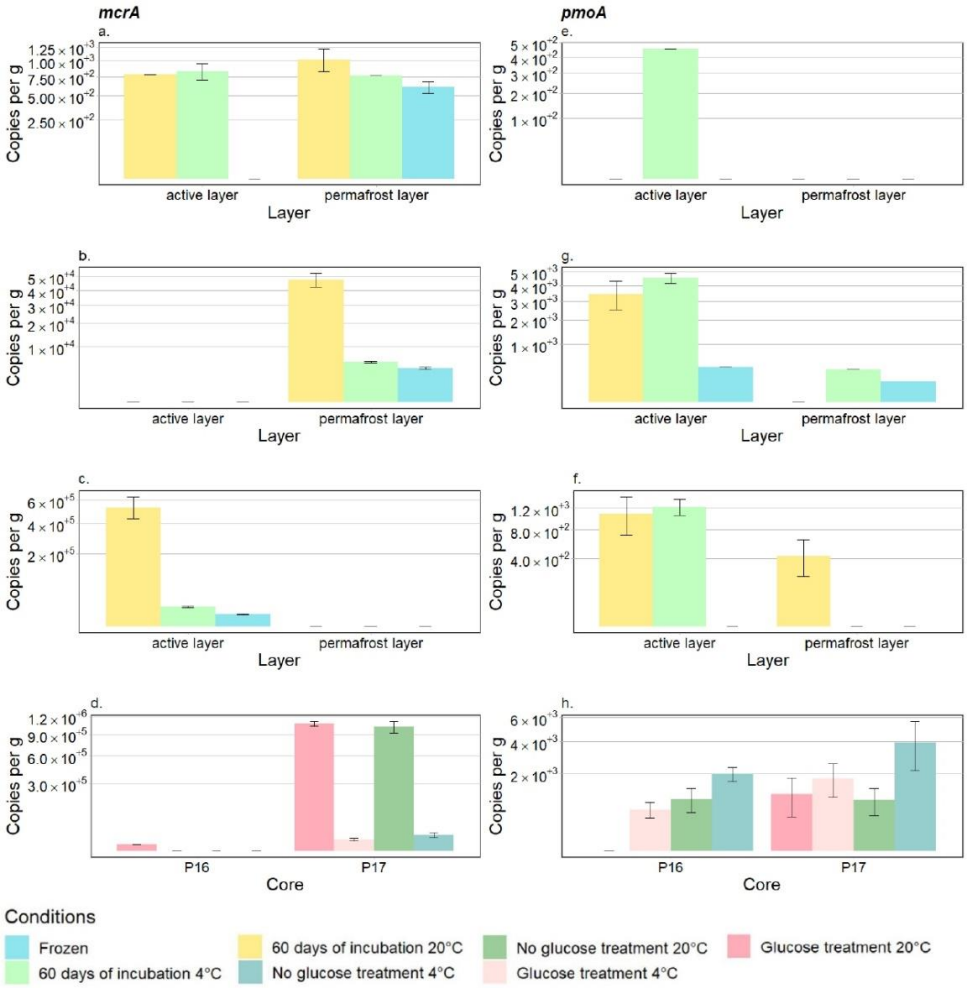
mcrA
pmoA
a.
b.
c.
d.
e.
f.
g.
h.
Copies per g
active layer
permafrost layer
Layer
P16
P17
Core
Conditions
Frozen
60 days of incubation 4°C
60 days of incubation 20°C
No glucose treatment 4°C
No glucose treatment 20°C
Glucose treatment 4°C
Glucose treatment 20°C

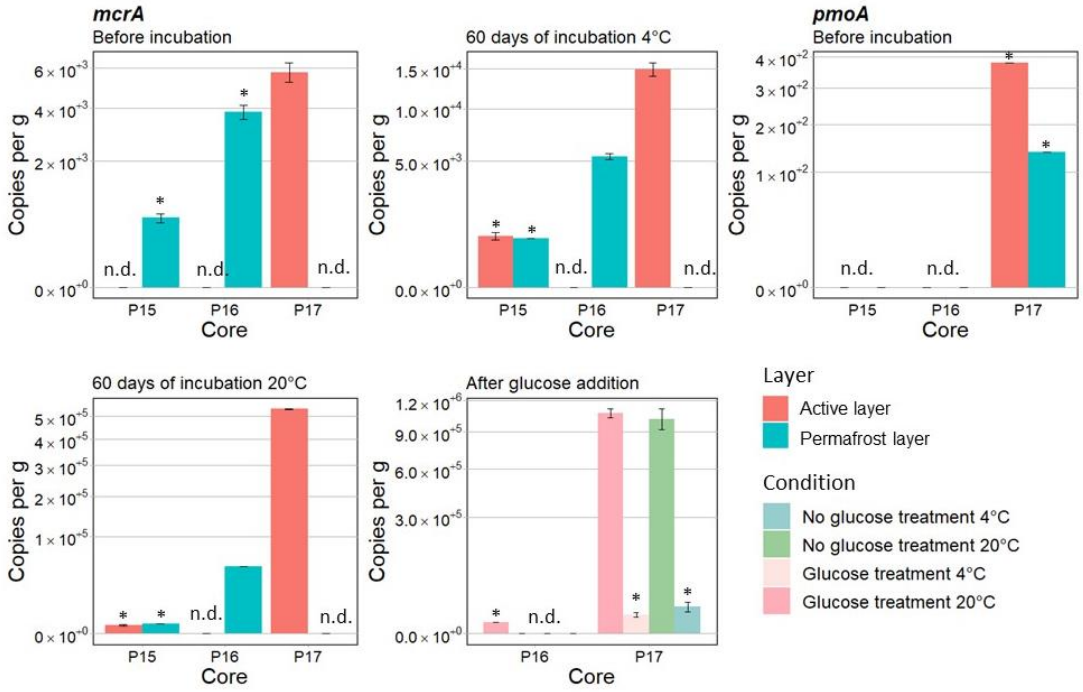

Figure 4: Means of copies per gram calculated with qPCR amplification at different times, for different conditions - before the incubation ~~(frozen),~~ after 60 days of incubation, and at the end. Gene copy numbers of *mcrA* were calculated for ~~(a.)~~ P15, ~~(b.) (~~P16), and ~~(c.)~~ P17. *mcrA* results for the active layers of P16 and P17 with or without glucose treatment after 67 days of incubation (d.). Gene copy numbers of *pmoA* are shown for ~~(e.)~~ P15, ~~(f.)~~ P16, and ~~(g.)~~ P17~~. (h.) *pmoA* results for~~ before the ~~active layers of P16 and P17 with or without glucose treatment after 67 days of~~ incubation. ~~Absence of values for some~~ Samples below detection limit are indicated by * and samples ~~is due to either low DNA concentration or failure in qPCR run~~where copies per gram were not detected are indicated by n.d.. Scale is expressed as square root in order to have a better display.

Formatted: Font: Italic

4. ~~4~~ Discussion

Formatted: Outline numbered + Level: 1 + Numbering Style: 1, 2, 3, … + Start at: 4 + Alignment: Left + Aligned at: 0 cm + Indent at: 0,63 cm

4.1 ~~Overview of different~~ CH_4 production in floodplain environment VS Yedoma cores

4.1.1 Different behaviors ~~in GHG production~~between landscape position

Formatted: Heading 3

4.1.1~~.~~1. Floodplain core

Formatted: Normal

We mimicked potential CH_4 production during a growing season in a floodplain environment of Kurungnakh Island in the Lena River Delta, and extended the incubation time to one year to capture the CH_4 production behavior. Within the first two months, the results showed high rates and quick onset of CH_4 production as well as presence of methanogen communities (Figure 4) in the active layer of the floodplain core P17 at 20°C only. Those findings, as well as the low CO_2~~ production under anaerobic~~:CH_4 ratio, indicated a quick establishment of optimum methanogenic conditions within the growing season time frame of 60 days (Symons and Buswell, 1993) (Figure 2c, Figure 3, Table 3Table 2). Herbst, (2022) did a similar incubation study with samples from the active floodplains of Kurungnakh Island and nearby Samoylov Island (Figure 1). CH_4 was produced from two of the three cores within the first 60 days of incubation (Supplementary Table 3). In both this study and the Herbst study, CH_4 production was triggered quickly after the beginning of incubation (from 10 to 40 days) from these

floodplain samples. Thus, these Arctic floodplain environments may allow the fast establishment of methanogens, and therefore, rapid CH_4 production under anaerobic conditions.

~~Anaerobic CO_2 production occurred in all the samples, and was similar throughout the cores, except for the frozen layer of P17. CO_2 production was slightly higher in the active layer than in the permafrost layer at 20°C only (Table 3, Figure 3). However, overall, none of the variables (landscape position, depth, or temperature) impacted CO_2 production.~~

~~Nevertheless, CO_2 production followed trends in total C and N contents. Indeed, all the samples, except P17-F, had similar C and N contents with values high enough to provide C mineralization (Strauss et al., 2013). In addition, the same samples produced comparable ranges of CO_2 during incubation (Table 1; Supplementary Table 1). Likewise, the frozen layer of P17 showed very low TOC and N contents as well as low CO_2 production throughout the incubation.~~

~~Under anoxic conditions, CO_2 is mainly produced by processes like denitrification or sulfate reduction (Conrad, 1989; Keller and Bridgham, 2007) rather than methanotrophy, which explains why the qPCR results for methanotrophic bacteria and methanogens were very low for P15 and P16 (Figure 4) (Liebner and Wagner, 2007). However, in core P17, the CO_2:CH_4 production ratio, as well as the presence of high number of methanogenic archaea (Table 2;~~ However, not all floodplain soils showed fast establishment of methane communities and high rates of potential methane production. Unlike the active layer, the permafrost layers of floodplain did not produce CH_4 after one year incubation at either 4°C and 20°C, and were still considered in the lag phase. The absence of detection of *mcrA* copy numbers per gram after 60-day incubation were below detection limits, indicating absence of methanogen communities in the permafrost samples (Figure 4~~), indicated that CO_2 was mainly produced by anaerobic respiration from methanogenesis (Symons and Buswell, 1993; Knoblauch et al., 2018; Holm et al., 2020). Unlike CH_4, anaerobic CO_2 production can be caused by several diverse anaerobic respiration pathways (Elderfield and Schlesinger, 1998) and mostly depends on C and N content (Knoblauch et al., 2018; Holm et al., 2020), which we observed in our results as well.~~

~~In order to simulate effects of root exudates or fresh C, we added glucose. After the addition of glucose, a slight increase of anaerobic CO_2 production at 20 °C was shown for P15 and P16. Nevertheless, glucose generally stimulates CO_2 production more efficiently under aerobic conditions than under anaerobic conditions (Yavitt et al., 1997; Pegoraro et al., 2019). This may explain the unexpectedly small effect of glucose on CO_2 production. Knoblauch et al. (2018) also noticed the small impact of glucose addition on CO_2 and CH_4 production under anaerobic conditions. In addition, the small effect of glucose treatment on CO_2 production supports the dependence of CO_2 production on C and N contents.~~

~~High CO_2 production rates were shown at the beginning of incubation for all the samples, following by an abrupt decrease. These CO_2 peaks are consistent with other studies which have also observed high CO_2 production at the beginning of incubation (Lee et al., 2012; Knoblauch et al., 2013; Yang et al., 2021). The rapid C turnover is caused by labile OM immediately available to microbial degradation at the beginning of incubation (Lee et al., 2012; Knoblauch et al., 2013; Yang et al., 2021). High CO_2 production in the beginning may also be related to the thawing of samples. Indeed, freeze-thaw activities improve the loss of soil organic carbon (SOC). The additional SOC is caused by the lysis of dead microbes already present inside the samples (Wang and Bettany, 1993).~~

~~**4.1.2 CH_4 production during short-term incubation**~~

~~In contrast to CO_2, high CH_4 production was detected for only one core, P17, at 20 °C. Under these conditions, the lag time was substantially reduced and core P17 produced CH_4 in both the active layer and the permafrost layer (Figure 3, Figure 3b). In addition, our results indicated a greater CH_4 production rate in the active layer than in the permafrost, which is consistent with other studies indicating higher production rates in the active layer than in the permafrost layer (Yavitt et al., 2006; Treat et al., 2015). Unlike P17, both P15 and P16 produced a low quantity of CH_4 during incubation at both 4 °C and 20 °C (Figure 3, Figure 3b). Even though total CH_4 production was greater at 4 °C than at 20 °C for these cores, CH_4 production was still considered very low (below the blanks; data not shown) and in lag phase.~~

Formatted: Highlight

~~Knoblauch et al. (2018) also observed long and heterogeneous lag times at 4°C for mineral soils (from 53±23 to up to 2500 days). They explained the long lag time by a lack of methanogens, or a lack of active methanogenic communities in soil samples, which is also applicable to short-term incubations. Lag time is the time required for methanogenic communities to be established in soil. In our study, results from the qPCR analysis supported this theory by showing low methanogen concentrations over the incubation period and no significant distinctions between 4 °C and 20 °C for P15 and P16 (Figure 4a; Figure 4b). Regarding the active layer of P17, high *mcrA* copies per gram of soil were measured over time (Figure 4), with greater concentration at 20°C than 4°C, which is consistent with Knoblauch et al.'s (2018) conclusions concerning lag time and the observed high CH_4 production in this study. Additionally, the high CO_2 production in P17 indicated active and abundant microbial communities which corresponds to high copy numbers of methanogens (Table 3, Figure 3; Figure 4c).~~

~~Our results showed the absence of a glucose effect on CH_4 production rates and on P15 and P16 microbial communities even after the second injection, indicating that the small CH_4 production observed was linked to microbe activities rather than to C availability. Regarding P17, we explain the absence of a visible glucose effect by an already high level of CH_4 production and overall methanogenic activities. This shows that in mineral soils, glucose is not the factor driving CH_4 production.~~

~~Overall, this study highlights two different CH_4 production behaviors among cores. High rates and quick onset of CH_4 production, as well as temperature sensitivity of CH_4 production in core P17. Temperature sensitivity is supported by Q10 values (Table 2) and by qPCR analysis (Figure 4), where methanogens were more abundant at 20 °C. Results from Ganzert et al. (2007) also showed that CH_4 was produced after one week in floodplain sediments, with greater production rates at higher temperature. In addition, the CO_2: CH_4 ratio for the P17 active layer at 20°C indicates the establishment of optimum methanogenic conditions by day 40 of this experiment (Symons and Buswell, 1993) (Table 2; Figure 2c). In contrast, P15 and P16 lagged behind, due to no established methanogenic communities. Even with the addition of glucose both CH_4 production and methanogen communities remained below detection limits (Figure 4, Table 2), which supports the lack of active methanogens in these two cores and indicates that the topographic position of the cores is an important factor to consider.~~

~~4.2~~). Similarly, low rates of CO_2 production, low C content, and high sand content in this sample indicate difficult conditions for many types of soil microbes in this permafrost sample (Figure 2, Figure 4, Table 1).

As expected, our results showed significant differences between CH_4 production rates at 4 and 20°C. At 4°C, almost 300-days of incubation were needed to trigger CH_4 production in the active layer of the floodplain (versus 14 days at 20°C), with a total cumulative CH_4 production four times lower than at 20°C (Figure 3). Other studies showed similar patterns, e.g., CH_4 production increases with temperature, and lag time is reduced (Ganzert et al., 2007; Treat et al., 2015). This is explained by a strong temperature sensitivity of methanogen communities (Westermann, 1993; Li et al., 2015). At the end of the growing season simulation, our results showed the *mcrA* copy numbers 36 times lower at 4°C than at 20°C (Figure 4), again indicating that the methanogen community required both time and warm temperatures to establish.

4.1.1.2. Yedoma cores

This study highlights a different CH_4 production behavior between the floodplain and the Yedoma cores. The permafrost layers from the Yedoma cores at 20°C only started producing CH_4 after six months of incubation, whereas the floodplain core produced CH_4 earlier (Figure 2). However, the CO_2:CH_4 ratios remained high after one year of incubation (Table 2), meaning that the methanogenic conditions are not yet optimum (Symons and Buswell, 1993). The low mCRA copies after the 60 – day incubation compared to the active layer of the floodplain, as well as the long lag times showed that the methanogen communities took more time to activate in the permafrost Yedoma cores (Figure 2, Figure 4).

Our results indicated higher CH_4 production rates in the permafrost layer than in the active layer, while others generally show the opposite (Yavitt et al., 2006; Treat et al., 2015, p.201). However, most of the studies which have worked on CH_4 production from Yedoma cores, showed high discrepancies in the cumulative CH_4 production. As explained above, lag time highly differed, as well as CH_4 production rates (Lee et al., 2012; Knoblauch et al., 2013; Walz et al., 2018; Jongejans et al., 2021).

It is therefore hard to estimate the potential production of CH_4 after thaw from Yedoma soils. Methanogen are high constrained microbial communities, and therefore the community size highly varies across the sites, which partly explains the discrepancies among the studies by the narrowness of the methanogen communities (Ernakovich et al., 2022).

The active layers at 4°C and 20deg C and permafrost layers at the lower temperatures were still in lag phase after one year incubation (Figure 2, Figure 3, Table 3). which is in line with the absence of detected methanogen community (Figure 4). Several multiannual studies observed also long and heterogeneous lag times at 4°C for Yedoma soils (from 53±23 to up to 2500 days; Knoblauch et al., 2018; Walz et al., 2018). Knoblauch et al., (2018) explained the long lag time by a lack of methanogens, or a lack of active methanogenic communities in soil samples. We added glucose to test whether the absence of CH_4 production was due to a lack of labile C or to a lack of established methanogenic communities. If the methanogen community was small, but established, we would expect to have community growth after the glucose addition. Since, glucose had no effect neither on CH_4 production rates nor on P15 and P16 microbial community growth, we concluded that the absence of CH_4 production for those samples was because the methanogens were not active (or not active enough to detect). It has been shown that the establishment of microbial community after thaw were correlated to the community characteristics as well as the thaw disturbance. For narrow microbial communities, like methanogen, stochastic processes strongly influence the abundances and activation of the microbial communities. After an abrupt thaw, like we simulated in our incubation study, the role played by stochastic processes on constrained microbial communities is even stronger (Deng et al., 2015; Ernakovich et al., 2022). Therefore, although we carried out incubation under anaerobic conditions, the quantity and the establishment of active methanogen community samples after thaw was strongly controlled by stochastic processes.

4.1.2. Controls on CH_4 production ~~under anaerobic conditions~~

Formatted: Heading 3

~~The results from soil characteristics showed that the quantity (TOC) and the quality (C:N) of organic C were in the range of Yedoma deposits and favourable to C mineralization (Zimov et al., 2006) for all the samples (Table 2). Soil characteristics showed little difference between samples (except for P17-F) (Table 1), hence, they were not able to explain differences in C production between P15 – P16 and P17 (Figure 3a).~~

~~We therefore hypothesized that landscape position rather than soil characteristics played a key role in the establishment of microbe activities and, consequently, explained variations in GHG production. Regular flooding of P17 and/or a high water table likely favors the conditions for methanogenesis. Indeed, the methanogen concentration before incubation showed the highest numbers in the floodplain (Figure 4c). Water saturation allows the establishment of anoxic conditions (Yavitt et al., 2006) and, therefore, better development of methanogens (Chasar et al., 2000; Paul et al., 2006; Jaatinen et al., 2007; Keller and Bridgham, 2007). In our case, oxidation marks or redox features were found in the depth profile of core P17, indicating periodic water saturation under in situ conditions. On the contrary, drier, well-drained conditions in the upland and the slope inhibit methanogenesis (Megonigal and Schlesinger, 2002). Here we found that a low methanogen concentration existed before incubation and there was little change in methanogen quantity after 60 days of incubation (Figure 4a,~~ CH_4 productions over the incubation time were not correlated to the TOC and TN% (Figure 3, Table 2) The landscape position rather than soil characteristics played a key role in the establishment of microbe activities and, consequently, explained variations in GHG production. On the first hand, periodic water saturation in core P17 was indicated by redox features that were found at depth, indicating some periodically anoxic conditions that likely favoured the methanogen communities (Chasar et al., 2000; Paul et al., 2006; Jaatinen et al., 2007; Keller and Bridgham, 2007) and allows short lag times prior to CH_4 production under anaerobic conditions (Figure 2, Table 3). On the other hand, well-drained conditions were found in the field for the active layers of both, the upland and the slope, that did not produce methane after one-year incubation (Figure 2, Figure 3). The aerobic condition due to the dry environment likely inhibited methanogenesis (Megonigal and Schlesinger, 2002). We quantified methanotroph communities to include more information about the potential for methane oxidation under field conditions, however the results are mainly either below detection or were not detected before the incubation (Figure 4~~b~~).

Formatted: Highlight

When we compare our results to another incubation study (Herbst, 2022) which was carried out using samples from Kurungnakh Island and nearby Samoylov Island (Figure 1), we found similar results. In the study by Herbst (2022), soil samples were collected in three different floodplains and incubated for 60 days at 20°C in both aerobic and anaerobic conditions. Under anaerobic conditions, CH_4 was produced from two of the three cores within 60 days of incubation (Supplementary Table 2). After 60 days the active layer of the most active floodplain studied by Herbst (2022) ranged around 5 µg C- CH_4.g C^{-1}.d^{-1}, compared to 90 µg C- CH_4.g C^{-1}.d^{-1} for the active layer of P17. Even if rates from similar floodplains are lower than what we found, CH_4 production was triggered quickly after the beginning of incubation (from 10 to 40 days). These results show that floodplain environments allow rapid CH_4 production after permafrost thaw under anaerobic conditions due to the fast establishment of methanogens. Therefore, the results support rapid establishment of microbes in floodplains under suitable redox conditions. These results are in line with our hypothesis concerning the impact of landscape position, e.g. periodically flooded areas provide suitable redox conditions for methanogenesis compared to drier areas. They also support initially anoxic conditions which trigger CH_4 production, while more aerobic conditions in the landscape coincide with a poor establishment of methanogenesis even when incubation conditions become favourable for methanogens.

Other in situ studies showed similar high CH_4 production in floodplains compared to drier sites with low CH_4 production (Huissteden, van et al., 2005; Oblogov et al., 2020). On the one hand, Oblogov et al. (2020) explained high CH_4 production by wetter conditions due to the floodplain location. On the other hand, Huissteden, van et al. (2005), argued that the high water table position could be the only wetness condition that could enhance CH_4 fluxes. In our case, no water table was reached when we cored P17; thus, we conclude that a high water table is not a necessary requirement and periodic flooding can enhance CH_4 production as well. Huissteden, van et al. (2005) also hypothesized that nutrient supply during flooding could stimulate methanogens. However, not all floodplains are able to produce high CH_4 fluxes (Huissteden, van et al., 2005), and discrepancies between production rates and cumulative emissions of P17 on the one hand, and the data by Herbst (2022) on the other highlight these high heterogeneities regarding CH_4 production in floodplains (Supplementary Table 2). Furthermore, settings that lead to high CH_4 conditions in floodplains are not fully understood (Huissteden, van et al., 2005) and need further investigations.

In addition to the topographic position, Holm et al. (2020) pointed out that paleoenvironmental conditions strongly drive CH_4 production by controlling the establishment of methanogen community. They showed that if paleoenvironmental conditions of soil deposition were favorable to CH_4 production, CH_4 production during thawing of permafrost, thousands of years later, would be higher than if paleoenvironmental conditions were unfavorable. Our analysis showed a strong dependence on landscape position in the control of C to CH_4 mineralization. Moreover, this partly explains the high heterogeneities observed in C production in small areas. Holm et al. (2020) also mentioned the influence of actual environmental conditions on the activity of methanogens. We therefore conclude that even if paleoenvironmental conditions influence the establishment of methanogens after permafrost thaw, suitable actual wetness conditions due to landscape position are an additional control on CH_4 production.

4.3). These results confirm our hypothesis concerning the impact of landscape position on CH_4 production: aerobic conditions in the landscape coincide with a poor establishment of methanogenesis even when incubation conditions become favourable for methanogens.

Unlike the active layers, the permafrost layers of Yedoma showed low but existing *mcrA* results from the Yedoma permafrost layers at 20°C (Figure 4), and started producing CH_4 after six months. The methanogen community was likely established prior or during the deposit of the Yedoma sediments and the microbial community survived although it was freeze-locked (Holm et al 2020).

4.2. Controls on potential CO_2 production

Our rates of CO_2 production per g C were in the same order of magnitude as other Yedoma incubation studies from Kurungnakh Island (Knoblauch et al., 2013, 2018) and nearby Lena Delta River (Walz et al., 2018). Like those studies, CO_2 production showed significantly higher CO_2 production per gram C than per gram DW (15 times higher), indicating labile C (Figure 2, Supplementary Fig 3). These similar results suggest that C in these Yedoma soils is easily available due to the organic-rich characteristics (Strauss et al., 2013). On the other hand, the adjacent samples from the permafrost layers of the floodplain showed CO_2 production g per C similar to the Yedoma cores while g per DW, it has the lowest cumulative production. Although floodplain environments in the Lena Delta are considered as a low C pool (Siewert et al., 2016), our results showed high C lability. The CO_2 production followed trends in total C and N contents. The samples with similar C and N contents produced comparable ranges of CO_2, whereas the sample (P17-F) with the lowest TOC and N content showed low CO_2 production (gram per DW) during incubation (Figure 2, Table 2, Supplementary Table 2). As shown by Schaedel et al (2014), the C:N ratio was positively correlated to the cumulative CO_2 production. However, the correlation was stronger at 4°C than 20°C (Supplementary Fig 7). Therefore, as proved by other studies (Schädel et al., 2014; Knoblauch et al., 2018), the quality (N), quantity (C), and the bioavailability (C:N) of the OM is a key factor for the mineralization into CO_2 production.

Our CO_2 and CH_4 production results combined with microbial analysis indicated that CO_2 production pathways might change according to the landscape position. The 1:1 CO_2:CH_4 production ratio, as well as the presence of high number of methanogenic archaea, indicated that the CO_2 production in the active layer floodplain could have come from methanogenesis (Figure 3, Figure 4) (Symons and Buswell, 1993; Knoblauch et al., 2018; Holm et al., 2020). In drier environments, like the P15 and P16 cores, the high CO_2:CH_4 production rates resulted from other, undetermined anaerobic decomposition pathways. Anaerobic respiration is a common function and diverse microbial communities are able to decompose the OM to CO_2, therefore, active microbial community is not a limited factor for C mineralization into CO_2 (Elderfield and Schlesinger, 1998). Based on the positive correlation between C:N and the cumulative CO_2 (Supplementary Fig 7), and the broad microbial community able to produce CO_2, our CO_2 production is rather controlled by the quality (N) and the quantity (TOC) of the OM than the microbial communities (Knoblauch et al., 2018; Holm et al., 2020).

4.3. Implication for ~~carbon~~C feedback in Kurungnakh Island during growing season

Formatted: Heading 3

~~With climate change, Arctic environments will be subject to changes in moisture conditions, vegetation shifts, and increased active layer depth (Serreze et al., 2000; Hinzman et al., 2005; Myers-Smith et al., 2011). Changes will affect C mineralization differently, depending on landscape position. In our study we identified that CO_2 was produced quickly under anaerobic conditions. Treat et al. (2015) studied soils with C and N content similar to our soils, but their soils produced half of the CO2 produced by our samples (except for the permafrost layer of P17). However, in other studies that monitored CO_2 production from Yedoma soils, production rates under anaerobic conditions were in a range similar to ours (around 100 µg CO_2 C $gC^{-1}.d^{-1}$) (Knoblauch et al., 2018; Walz et al., 2018). These similar results suggest that C in these Yedoma soils is easily available due to the soil's organic-rich characteristics (Strauss et al., 2013). Therefore, our samples exhibited a high CO_2 production rate in short-term permafrost thaw experiments, indicating easily available C. However, the same studies, as well as Schädel et al. (2014), pointed out the small size of the labile C pool of Yedoma deposits and nearby soils on Kurungnakh Island (between 5% and 2% TOC content). Short-term incubation studies have relied mainly on the labile C pool (Schädel et al., 2014; Walz et al., 2018; Schädel et al., 2020); therefore, when the labile pool is depleted, carbon production rates likely remain low (Walz et al., 2018).~~

~~Our gas production results combined with microbial analysis indicated that CO_2 production pathways might change according to the landscape position. In floodplain environments, CO_2 production came essentially from methanogenesis (indicated by the 1:1 production ratio, Figure 3) whereas in drier environments, like the P15 and P16 cores, CO_2 production also resulted~~

~~from other, undetermined anaerobic decomposition pathways. Nevertheless, even if pathways were different, CO_2 production rates depend mostly on C and N contents (Schädel et al., 2014; Holm et al., 2020). Therefore, landscape position is not a major factor controlling CO_2 production compared to soil characteristics (Figure 5). The CO_2 production per gram soil (Supplementary Figure 1) supports this by showing lower CO_2 production for low TOC contents. However, the cumulative CO_2 production (per gram C) in the active layer of P17 was two to three time higher than in the other samples, although the other samples had similar C and N contents, with slightly lower N contents in P17 (Table 1). This means that the carbon in the active layer of P17 was more easily decomposed by microbes than the C in the other cores, and that the microbial communities were therefore more active. We suggest that those discrepancies were due to microbe community adaptations under anaerobic conditions. Even though anaerobic CO_2 pathways were established, microbes in P15 and P16 seemed to be less adapted to anaerobic conditions. This could be explained by better drained soils during permafrost thaw in summer for P15 and P16.~~

~~Unlike CO_2 production, CH_4 production is more dependent on landscape position, which triggers methanogenesis. We showed that samples from a floodplain were able to produce a high quantity of CH_4 in a short amount of time (less than 40 days) under anoxic conditions at 20°C. Our results and those of Herbst (2022) showed that the active layer of floodplain samples produced CH_4 in large quantity ($6.5x10^3$ µg CH_4-C.gC^{-1}). Nevertheless, even if CH_4 production in permafrost layers started after the production began in the active layers, permafrost layers were still capable of producing CH_4. Due to climate change, root exudates, or an additional supply of nutrients from sedimentation of particulate OM (Huissteden, van et al., 2005), will likely increase. In combination with active layer deepening, these landscape locations will maintain or even increase CH_4 production in floodplain active layers. Notwithstanding, it is likely that CH_4 emissions from floodplains could occur only during flooding periods. Incubation and in situ measurements have shown that in dry conditions CH_4 emissions from floodplain environments were significantly lower than under wet conditions (Huissteden, van et al., 2005; Oblogov et al., 2020). In contrast, even though this incubation experiment was carried out under anoxic conditions, active methanogenic communities were not able to establish themselves in samples from drier areas during a simulated short-term permafrost thaw (Table 3,~~ With climate change, Arctic environments will be subject to changes in moisture conditions, vegetation shifts, increased active layer depth and abrupt permafrost thaw (Serreze et al., 2000; Hinzman et al., 2005; Myers-Smith et al., 2011; Turetsky et al., 2019). Our permafrost thaw simulation under wet summer conditions in Kurungnakh Island showed that the CO_2 production for the Yedoma cores was similar in magnitude to other studies including Yedoma. Under incubation, all the Yedoma samples reached the maximum production rates within the first two months of incubation (Figure 2). Schädel et al., (2014) attributed the decrease in CO_2 production rates after some time in incubations to a rapid C turnover that relied mainly on the decomposition of the labile C pool (Schädel et al., 2014; Walz et al., 2018; Schädel et al., 2020). However, several studies pointed out the small size of the labile C pool of Yedoma deposits (Knoblauch et al., 2013; Strauss et al., 2013b). Here, the Yedoma soils from Kurungnakh Island, showed labile C pool depletion after six months incubation (e.g., the CO_2 production rates decreased and the cumulative CO_2 production plateaued after six months incubation; Figure 2). Therefore, we supposed that under wet summer condition, it is likely to have a rapid C turnover, and CO_2 production during all the growing season.

The active layer of the floodplain at 20°C produced up to 300 µg CH_4-C.g^{-1}DW at the end of the simulated growing season. The low-lying position of the floodplain allows regular flooding from the river. Therefore, the hydrological conditions of this area provide favorable redox conditions, e.g., anaerobic conditions, for the establishment of active methanogen communities if the temperature is high enough. Long – term in situ measurements in the Lena Delta have shown the highest CH_4 emission rates for moist to dry dwarf dominated tundra, located mainly in lower floodplain environments (5048.5 mg m^{-2} a^{-1}; Schneider et al., 2009). In this Lena Delta area, CH_4 emissions have been measured from June to September with the highest emission rates in July. Therefore, we expected that our floodplain site study will turn into a net CH_4 source quickly after the beginning of the growing season.

While CH_4 production did occur in the year-long anaerobic incubation of Yedoma samples, other factors might result in these tundra regions still remaining a net CH_4 sink barring abrupt permafrost thaw or very low CH_4 emissions in CH_4 in these regions

(Schneider et al., 2009; Juncher Jørgensen et al., 2015). In these dry Yedoma sites, the net CH_4 flux is the balance between CH_4 production in anoxic soil layers and CH_4 oxidation in overlying aerobic layers. Here, we showed that CH_4 production is possible with a long lag time given high enough temperatures (Figure 2, Figure 3, Table 3). Therefore, based on our results it is unlikely that the upland and the slope from this area, on Kurungnakh Island, establish active methanogen communities during the growing season although the active layer might deepen, soil moisture might increases, and even though C in Yedoma sediments is highly bioavailable (Anthony et al., 2014; Mann et al., 2014; Spencer et al., 2015). Nevertheless, under field conditions nutrients or organisms triggering methanogenesis can be transported, and hence, stimulate CH_4 production if there is anaerobic condition (Lara et al., 2019). The CH_4 oxidation in overlying surfaces seems to have inhibited CH_4 production in the active layers of the Yedoma samples (Figure 2; Figure 3~~, Figure 4, Figure 5). In addition, in ice-rich permafrost, water saturated conditions are maintained mostly by melt water, whereas floodplain soils are saturated with water from the rivers which carries nutrients and which likely stimulates microbial activities (King and Reeburgh, 2002b; Oblogov et al., 2020) . Therefore, even if areas like ice-rich tundra reach high water contents due to the thawing of permafrost-affected soils, it is unlikely that a methanotrophic community will be established during a short Arctic summer.~~

~~Our experimental study, combined with others, highlights the high potential of CH_4 emissions from Arctic floodplains and allows us to make C feedback predictions of changes in GHG production as a function of landscape position. High CH_4 emissions were measured in waterlogged (floodplain) areas while C emissions in uplands mainly came from CO_2 production (Huissteden, van et al., 2005; Treat et al., 2018; Oblogov et al., 2020; Hashemi et al., 2021) (Figure 5). Even though we could partly explain heterogeneities of GHG emissions from our incubated samples, it is still uncertain how climate change will impact C emissions under in situ conditions, or in other polar landscapes. Numerous variables and feedback loops such as vegetation, water table position, flooding time, or nutrient supply to floodplains are still understudied and, therefore, the understanding of C mineralization in permafrost affected floodplains is limited.~~

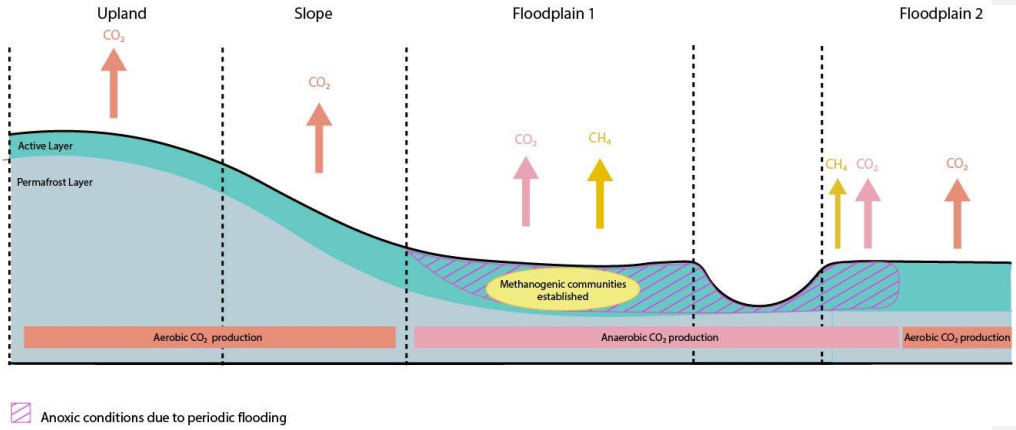

~~**Figure 5: Schematic figure of the studied transect in warming conditions. Gas emissions are represented according to the results found in this study.**~~

Formatted: Not Highlight

), but our methanotroph results did not allow us to draw conclusion. However, based on the site description, and the CH_4 production in the active layers of the Yedoma samples, it is likely that CH_4 oxidation happens in field conditions. Plant transport of CH_4 can allow it to bypass oxidation and is also likely a big factor in these sites. A recent study in Samoylov Island, Lena River Delta showed an increase of CH_4 emissions at the beginning of the growing season over the past twenty years in moist polygon tundra and attributed it to plant transport (Rößger et al., 2022). Therefore, CH_4 emissions from dry area could occur due to either a vegetation shift or earlier vegetation activity.

Our results showed a high CH_4 production potential from the floodplain, however, floodplain environments are periodically flooded, meaning there might be periods were the floodplain would be too dry to allow methane production (Huissteden et al., 2005; Oblogov et al., 2020). A long-term study like Rößger et al., (2022) in floodplains environments would help to quantify CH4 emissions from floodplains, how often it occurs during the growing season, and how the soil moisture will change over time.

5 Conclusion

~~In this study, links were made between landscape position, GHG production, and microbes. We observed that C releases as CO_2 and CH_4 can occur during short-term thawing of permafrost. CO_2 was produced in similar quantity from the upland and slope (between 2.2 9x10^3 µgCO_2-C.gC^{-1} and 3.39x10^3 µgCO_2-C.gC^{-1}), whereas the floodplain produced more than twice that amount (6.9x10^3 µgCO_2-C.gC^{-1}). In addition, our study showed that CH_4 lag time can be significantly reduced at higher soil temperature if the landscape position favours methanogenesis. Indeed, in a floodplain area 6.5x10^3 µgCH_4-C.gC^{-1} was produced, while in the upland and the slope only a slight quantity (<1 µgCH_4-C.gC^{-1}) was produced. However, comparisons with other studies showed high heterogeneities for C production in floodplain areas mainly related to wetness conditions (water table position or flooding events). Furthermore, C mineralization in floodplains is largely understudied; therefore, the quantity of in situ C emissions in the context of climate change remains unclear. It is, therefore, necessary to study the different parameters affecting moisture conditions in floodplains (water table position, frequency of flooding) as well as their relationships with microbial species and abundance, and the role of the vegetation in order to achieve a better understanding of processes impacting C losses from floodplains.~~In this study we provide new information regarding the importance of the landscape position to trigger CH_4 production during the growing season in Kurungnakh Island. High CH_4 production were measured in waterlogged (floodplain) areas within the 60 days simulation of the growing season at 20C, thanks to a fast establishment of the methanogen community (14 days). In contrast, the well-drained Yedoma samples were still in the lag phase at the end of the growing season simulation, and therefore, C turnover came from CO_2 production. CH_4 was produced by the Yedoma permafrost layers after a lag phase of six months at 20 °C. Although the permafrost layer of the floodplain had low TOC, we identified similar C lability for the three cores as for other studies with samples from Siberia, and therefore high potential C production throughout this region. As a result, the data presented in this case study contribute to quantify and understand C turnover in permafrost areas. Questions remain regarding how to upscale results from laboratory incubation to in-situ conditions, and our results highlighted the need to understand better changes in redox conditions throughout landscape position to improve the upscaling.

Author contributions

M.L. C.T. and S.L. designed the study. M.L. conducted all the experiments (soil analyses, incubations, and microbe quantification). M.F. and A.R. collected the soil samples and field notes during the expedition in 2018 and created the map. S.L. furnished laboratory materials to perform microbe analyses and gas measurements. T.H. provided data from her incubation experiments. M.L wrote the manuscript with contributions from all the co-authors.

Acknowledgments

Funding for this study was provided by ERC-H2020 #851181 FluxWIN, the Helmholtz Impulse Initiative and Networking Fund. Samples were collected during the joint Russian-German LENA 2018 expedition to Samoylov Island within the framework of the BMBF KoPf (Kohlenstoff in Permafrost) project (#3F0764B). This project was also supported by the European Erasmus+ programme. We thank the staff at the Samoylov Research Station for support and logistics during the fieldwork. We also thank the Alfred-Wegener Institute and GFZ lab technicians in Potsdam for laboratory assistance.

References

Adamczyk, M., Rüthi, J., and Frey, B.: Root exudates increase soil respiration and alter microbial community structure in alpine permafrost and active layer soils, Environmental Microbiology, 23, 2152–2168, https://doi.org/10.1111/1462-2920.15383, 2021.

AMAP: Arctic Climate Change Update 2021: Key Trends and Impacts. Summary for Policy-makers, 2021.

Angle, J. C., Morin, T. H., Solden, L. M., Narrowe, A. B., Smith, G. J., Borton, M. A., Rey Sanchez, C., Daly, R. A., Mirfenderesgi, G., Hoyt, D. W., Riley, W. J., Miller, C. S., Bohrer, G., and Wrighton, K. C.: Methanogenesis in oxygenated soils is a substantial fraction of wetland methane emissions, Nat Commun, 8, 1567, https://doi.org/10.1038/s41467-017-01753-4, 2017.

Anthony, K. M. W., Zimov, S. A., Grosse, G., Jones, M. C., Anthony, P. M., Iii, F. S. C., Finlay, J. C., Mack, M. C., Davydov, S., Frenzel, P., and Frolking, S.: A shift of thermokarst lakes from carbon sources to sinks during the Holocene epoch, Nature, 511, 452–456, https://doi.org/10.1038/nature13560, 2014.

Boike, J., Kattenstroth, B., Abramova, K., Bornemann, N., Chetverova, A., Fedorova, I., Fröb, K., Grigoriev, M., Grüber, M., Kutzbach, L., Langer, M., Minke, M., Muster, S., Piel, K., Pfeiffer, E.-M., Stoof, G., Westermann, S., Wischnewski, K., Wille, C., and Hubberten, H.-W.: Baseline characteristics of climate, permafrost and land cover from a new permafrost observatory in the Lena River Delta, Siberia (1998–2011), Biogeosciences, 10, 2105–2128, https://doi.org/10.5194/bg-10-2105-2013, 2013.

Bruhwiler, L., Dlugokencky, E., Masarie, K., Ishizawa, M., Andrews, A., Miller, J., Sweeney, C., Tans, P., and Worthy, D.: CarbonTracker-CH_4: an assimilation system for estimating emissions of atmospheric methane, 14, 8269–8293, https://doi.org/10.5194/acp-14-8269-2014, 2014.

Callaghan, T. V., Bergholm, F., Christensen, T. R., Jonasson, C., Kokfelt, U., and Johansson, M.: A new climate era in the sub-Arctic: Accelerating climate changes and multiple impacts, Geophysical Research Letters, 37, https://doi.org/10.1029/2009GL042064, 2010.

Chasar, L. S., Chanton, J. P., Glaser, P. H., Siegel, D. I., and Rivers, J. S.: Radiocarbon and stable carbon isotopic evidence for transport and transformation of dissolved organic carbon, dissolved inorganic carbon, and CH4 in a northern Minnesota peatland, Global Biogeochemical Cycles, 14, 1095–1108, https://doi.org/10.1029/1999GB001221, 2000.

Conrad, R.: Control of Methane Productionmicrobial methane production in Terrestrial Ecosystems. In: Andreae, M.O.wetland rice fields, Nutrient Cycling in Agroecosystems, 64, 59–69, https://doi.org/10.1023/A:1021178713988, 2002.

Davidson, E. A. and Schimel, D.S., Eds., ExchangeJanssens, I. A.: Temperature sensitivity of Trce Gases between Terrestrial Ecosystemssoil carbon decomposition and the Atmosphere, Wiley, Chichester, 1989feedbacks to climate change, Nature, 440, 165–173, https://doi.org/10.1038/nature04514, 2006.

Dean, J. F., Middelburg, J. J., Röckmann, T., Aerts, R., Blauw, L. G., Egger, M., Jetten, M. S. M., de Jong, A. E. E., Meisel, O. H., Rasigraf, O., Slomp, C. P., in't Zandt, M. H., and Dolman, A. J.: Methane Feedbacks to the Global Climate System in a Warmer World, Rev. Geophys., 56, 207–250, https://doi.org/10.1002/2017RG000559, 2018.

DuttaDeng, J., Gu, Y., Zhang, J., Xue, K., Qin, Y., Yuan, M., Yin, H., He, Z., Wu, L., Schuur, E. aA. G., NeffTiedje, J. CM., and Zimov, S. A.: Potential carbon release fromZhou, J.: Shifts of tundra bacterial and archaeal communities along a permafrost soils of Northeastern Siberia, 12, 2336–2351thaw gradient in Alaska, Molecular Ecology, 24, 222–234, https://doi.org/10.1111/j.1365-2486.2006.01259.x, 2006mec.13015, 2015.

Douglas, T. A., Turetsky, M. R., and Koven, C. D.: Increased rainfall stimulates permafrost thaw across a variety of Interior Alaskan boreal ecosystems, npj Clim Atmos Sci, 3, 1–7, https://doi.org/10.1038/s41612-020-0130-4, 2020.

Elder, C. D., Thompson, D. R., Thorpe, A. K., Hanke, P., Walter Anthony, K. M., and Miller, C. E.: Airborne Mapping Reveals Emergent Power Law of Arctic Methane Emissions, Geophysical Research Letters, 47, e2019GL085707, https://doi.org/10.1029/2019GL085707, 2020.

Elderfield, H. and Schlesinger, W.: Biogeochemistry. An Analysis of Global Change, Earth System Science and Global Change., Geological Magazine, 135, 819–842, https://doi.org/10.1017/S0016756898231505, 1998.

~~Fox, J. F. and Cleve, K. V.: Relationships between cellulose decomposition, Jenny's k, forest floor nitrogen, and soil temperature in Alaskan taiga forests, Can. J. For. Res., 13, 789–794, https://doi.org/10.1139/x83-109, 1983.~~

~~Fuchs, M., Grosse, G., Jones, B. M., Strauss, J., Baughman, C. A., and Walker, D. A.: Sedimentary and geochemical characteristics of two small permafrost-dominated Arctic river deltas in northern Alaska, Arktos, 4, 1–18, https://doi.org/10.1007/s41063-018-0056-9, 2018.~~

Ernakovich, J. G., Barbato, R. A., Rich, V. I., Schädel, C., Hewitt, R. E., Doherty, S. J., Whalen, E. D., Abbott, B. W., Barta, J., Biasi, C., Chabot, C. L., Hultman, J., Knoblauch, C., Vetter, M. C. Y. L., Leewis, M.-C., Liebner, S., Mackelprang, R., Onstott, T. C., Richter, A., Schütte, U. M. E., Siljanen, H. M. P., Taş, N., Timling, I., Vishnivetskaya, T. A., Waldrop, M. P., and Winkel, M.: Microbiome assembly in thawing permafrost and its feedbacks to climate, Global Change Biology, 28, 5007–5026, https://doi.org/10.1111/gcb.16231, 2022.

Faucherre, S., Jørgensen, C. J., Blok, D., Weiss, N., Siewert, M. B., Bang-Andreasen, T., Hugelius, G., Kuhry, P., and Elberling, B.: Short and Long-Term Controls on Active Layer and Permafrost Carbon Turnover Across the Arctic, Journal of Geophysical Research: Biogeosciences, 123, 372–390, https://doi.org/10.1002/2017JG004069, 2018.

Fewster, R. E., Morris, P. J., Ivanovic, R. F., Swindles, G. T., Peregon, A. M., and Smith, C. J.: Imminent loss of climate space for permafrost peatlands in Europe and Western Siberia, Nat. Clim. Chang., 12, 373–379, https://doi.org/10.1038/s41558-022-01296-7, 2022.

Fuchs, M.: Soil organic carbon and nitrogen pools in thermokarst-affected permafrost terrain, phd, Universität Potsdam, 2019.

Ganzert, L., Jurgens, G., Münster, U., and Wagner, D.: Methanogenic communities in permafrost-affected soils of the Laptev Sea coast, Siberian Arctic, characterized by 16S rRNA gene fingerprints, FEMS Microbiology Ecology, 59, 476–488, https://doi.org/10.1111/j.1574-6941.2006.00205.x, 2007.

Grigoriev, M. N.: Cryomorphogenesis in the Lena Delta. Yakutsk, Permafrost Institute Press, 176 pp, 1993.

Hales, B. A., Edwards, C., Ritchie, D. A., Hall, G., Pickup, R. W., and Saunders, J. R.: Isolation and identification of methanogen-specific DNA from blanket bog peat by PCR amplification and sequence analysis, Applied and Environmental Microbiology, https://doi.org/10.1128/aem.62.2.668-675.1996, 1996.

~~Hamdi, S., Moyano, F., Sall, S., Bernoux, M., and Chevallier, T.: Synthesis analysis of the temperature sensitivity of soil respiration from laboratory studies in relation to incubation methods and soil conditions, Soil Biology and Biochemistry, 58, 115–126, https://doi.org/10.1016/j.soilbio.2012.11.012, 2013.~~

~~Hashemi, J., Zona, D., Arndt, K. A., Kalhori, A., and Oechel, W. C.: Seasonality buffers carbon budget variability across heterogeneous landscapes in Alaskan Arctic Tundra, Environ. Res. Lett., https://doi.org/10.1088/1748-9326/abe2d1, 2021.~~

Herbst, T.: Carbon ~~stocks~~Stocks and ~~potential greenhouse gas release~~Potential Greenhouse Gas Release of ~~permafrost~~Permafrost-affected ~~active floodplains~~Active Floodplains in the Lena River Delta, ~~Alfred-Wegener-Institute, Potsdam, Germany,~~master, Faculty of Environment and Natural Resources, 73 pp., 2022.

Hinzman, L. D., Bettez, N. D., Bolton, W. R., Chapin, F. S., Dyurgerov, M. B., Fastie, C. L., Griffith, B., Hollister, R. D., Hope, A., Huntington, H. P., Jensen, A. M., Jia, G. J., Jorgenson, T., Kane, D. L., Klein, D. R., Kofinas, G., Lynch, A. H., Lloyd, A. H., McGuire, A. D., Nelson, F. E., Oechel, W. C., Osterkamp, T. E., Racine, C. H., Romanovsky, V. E., Stone, R. S., Stow, D. A., Sturm, M., Tweedie, C. E., Vourlitis, G. L., Walker, M. D., Walker, D. A., Webber, P. J., Welker, J. M., Winker, K. S., and Yoshikawa, K.: Evidence and Implications of Recent Climate Change in Northern Alaska and Other Arctic Regions, Climatic Change, 72, 251–298, https://doi.org/10.1007/s10584-005-5352-2, 2005.

~~Hobbie, S. E.: Interactions between Litter Lignin and Soil Nitrogen Availability during Leaf Litter Decomposition in a Hawaiian Montane Forest, 3, 484–494, 2000.~~

Holm, S., Walz, J., Horn, F., Yang, S., Grigoriev, M. N., Wagner, D., Knoblauch, C., and Liebner, S.: Methanogenic response to long-term permafrost thaw is determined by paleoenvironment, FEMS Microbiology Ecology, 96, https://doi.org/10.1093/femsec/fiaa021, 2020.

Hugelius, G., Strauss, J., Zubrzycki, S., Harden, J. W., Schuur, E. a. G., Ping, C.-L., Schirrmeister, L., Grosse, G., Michaelson, G. J., Koven, C. D., O'Donnell, J. A., Elberling, B., Mishra, U., Camill, P., Yu, Z., Palmtag, J., and Kuhry, P.: Estimated stocks of circumpolar permafrost carbon with quantified uncertainty ranges and identified data gaps, Biogeosciences, 11, 6573–6593, https://doi.org/10.5194/bg-11-6573-2014, ~~2014~~2014a.

Hugelius, G., Strauss, J., Zubrzycki, S., Harden, J. W., Schuur, E. a. G., Ping, C.-L., Schirrmeister, L., Grosse, G., Michaelson, G. J., Koven, C. D., O'Donnell, J. A., Elberling, B., Mishra, U., Camill, P., Yu, Z., Palmtag, J., and Kuhry, P.: Estimated stocks of circumpolar permafrost carbon with quantified uncertainty ranges and identified data gaps, Biogeosciences, 11, 6573–6593, https://doi.org/10.5194/bg-11-6573-2014, 2014b.

Huissteden, J. van, Maximov, T. C., and Dolman, A. J.: High methane flux from an arctic floodplain (Indigirka lowlands, eastern Siberia): methane flux arctic floodplain Siberia, J. Geophys. Res., 110, n/a-n/a, https://doi.org/10.1029/2005JG000010, 2005.

IPCC: IPCC, 2021: Climate Change 2021: The Physical Science Basis. Contribution of Working Group I to the Sixth Assessment Report of the Intergovernmental Panel on Climate Change, Cambridge University Press. In Press., 2021.

Jaatinen, K., Fritze, H., Laine, J., and Laiho, R.: Effects of short- and long-term water-level drawdown on the populations and activity of aerobic decomposers in a boreal peatland, Global Change Biology, 13, 491–510, https://doi.org/10.1111/j.1365-2486.2006.01312.x, 2007.

Jongejans, L. L., Liebner, S., Knoblauch, C., Mangelsdorf, K., Ulrich, M., Grosse, G., Tanski, G., Fedorov, A. N., Konstantinov, P. Ya., Windirsch, T., Wiedmann, J., and Strauss, J.: Greenhouse gas production and lipid biomarker distribution in Yedoma and Alas thermokarst lake sediments in Eastern Siberia, Global Change Biology, 27, 2822–2839, https://doi.org/10.1111/gcb.15566, 2021.

Juncher Jørgensen, C., Lund Johansen, K. M., Westergaard-Nielsen, A., and Elberling, B.: Net regional methane sink in High Arctic soils of northeast Greenland, Nature Geosci, 8, 20–23, https://doi.org/10.1038/ngeo2305, 2015.

Keller, J. K. and Bridgham, S. D.: Pathways of anaerobic carbon cycling across an ombrotrophic-minerotrophic peatland gradient, Limnology and Oceanography, 52, 96–107, https://doi.org/10.4319/lo.2007.52.1.0096, 2007.

~~King, J. Y. and Reeburgh, W. S.: A pulse-labeling experiment to determine the contribution of recent plant photosynthates to net methane emission in arctic wet sedge tundra, Soil Biology and Biochemistry, 34, 173–180, https://doi.org/10.1016/S0038-0717(01)00164-X, 2002a.~~

~~King, J. Y. and Reeburgh, W. S.: A pulse-labeling experiment to determine the contribution of recent plant photosynthates to net methane emission in arctic wet sedge tundra, Soil Biology and Biochemistry, 34, 173–180, https://doi.org/10.1016/S0038-0717(01)00164-X, 2002b.~~

Knoblauch, C., Beer, C., Sosnin, A., Wagner, D., and Pfeiffer, E.-M.: Predicting long-term carbon mineralization and trace gas production from thawing permafrost of Northeast Siberia, Global Change Biology, 19, 1160–1172, https://doi.org/10.1111/gcb.12116, 2013.

Knoblauch, C., Beer, C., Liebner, S., Grigoriev, M. N., and Pfeiffer, E.-M.: Methane production as key to the greenhouse gas budget of thawing permafrost, Nature Climate Change, 8, 309–312, https://doi.org/10.1038/s41558-018-0095-z, 2018.

~~Koch, K., Knoblauch, C., and Wagner, D.: Methanogenic community composition and anaerobic carbon turnover in submarine permafrost sediments of the Siberian Laptev Sea, 11, 657–668, https://doi.org/10.1111/j.1462-2920.2008.01836.x, 2009.~~

Koven, C. D., Ringeval, B., Friedlingstein, P., Ciais, P., Cadule, P., Khvorostyanov, D., Krinner, G., and Tarnocai, C.: Permafrost carbon-climate feedbacks accelerate global warming, PNAS, 108, 14769–14774, https://doi.org/10.1073/pnas.1103910108, 2011.

Kuhn, M. A., Thompson, L. M., Winder, J. C., Braga, L. P. P., Tanentzap, A. J., Bastviken, D., and Olefeldt, D.: Opposing Effects of Climate and Permafrost Thaw on CH4 and CO2 Emissions From Northern Lakes, AGU Advances, 2, e2021AV000515, https://doi.org/10.1029/2021AV000515, 2021.

Kuhry, P., Bárta, J., Blok, D., Elberling, B., Faucherre, S., Hugelius, G., Jørgensen, C. J., Richter, A., Šantrůčková, H., and Weiss, N.: Lability classification of soil organic matter in the northern permafrost region, Biogeosciences, 17, 361–379, https://doi.org/10.5194/bg-17-361-2020, 2020.

Lara, M. J., Lin, D. H., Andresen, C., Lougheed, V. L., and Tweedie, C. E.: Nutrient Release From Permafrost Thaw Enhances CH4 Emissions From Arctic Tundra Wetlands, Journal of Geophysical Research: Biogeosciences, 124, 1560–1573, https://doi.org/10.1029/2018JG004641, 2019a.

Lara, M. J., Lin, D. H., Andresen, C., Lougheed, V. L., and Tweedie, C. E.: Nutrient Release From Permafrost Thaw Enhances CH4 Emissions From Arctic Tundra Wetlands, Journal of Geophysical Research: Biogeosciences, 124, 1560–1573, https://doi.org/10.1029/2018JG004641, 20192019b.

Lee, H., Schuur, E. A. G., Inglett, K. S., Lavoie, M., and Chanton, J. P.: The rate of permafrost carbon release under aerobic and anaerobic conditions and its potential effects on climate, Global Change Biology, 18, 515–527, https://doi.org/10.1111/j.1365-2486.2011.02519.x, 2012.

LiebnerLi, F., Tianze, S.,, and Wagner, D.: Abundance, distribution and potential activityYahai, L.: Snapshot of methane oxidizing bacteriamethanogen sensitivity to temperature in permafrost soilsZoige wetland from the Lena Delta, Siberia, 9, 107–117Tibetan plateau, Frontiers in Microbiology, https://doi.org/10.1111/j.1462-2920.2006.01120.x, 20073389/fmicb.2015.00131, 2015.

Liebner, S., Ganzert, L., Kiss, A., Yang, S., Wagner, D., and Svenning, M. M.: Shifts in methanogenic community composition and methane fluxes along the degradation of discontinuous permafrost, Frontiers in Microbiology, 6, 2015.

Lupascu, M., Wadham, J. L., Hornibrook, E. R. C., and Pancost, R. D.: Temperature Sensitivity of Methane Production in the Permafrost Active Layer at Stordalen, Sweden: A Comparison with Non-permafrost Northern Wetlands, 44, 469–482, https://doi.org/10.1657/1938-4246-44.4.469, 2012.

Mackelprang, R., Waldrop, M. P., DeAngelis, K. M., David, M. M., Chavarria, K. L., Blazewicz, S. J., Rubin, E. M., and Jansson, J. K.: Metagenomic analysis of a permafrostMann, P. J., Sobczak, W. V., LaRue, M. M., Bulygina, E., Davydova, A., Vonk, J. E., Schade, J., Davydov, S., Zimov, N., Holmes, R. M., and Spencer, R. G. M.: Evidence for key enzymatic controls on metabolism of Arctic river organic matter, Global Change Biology, 20, 1089–1100, https://doi.org/10.1111/gcb.12416, 2014.

McCalley, C. K., Woodcroft, B. J., Hodgkins, S. B., Wehr, R. A., Kim, E.-H., Mondav, R., Crill, P. M., Chanton, J. P., Rich, V. I., Tyson, G. W., and Saleska, S. R.: Methane dynamics regulated by microbial community reveals a rapid response to permafrost thaw, Nature, 480, 368–371514, 478–481, https://doi.org/10.1038/nature10576, 2011nature13798, 2014.

Megonigal, J. P. and Schlesinger, W. H.: Methane-limited methanotrophy in tidal freshwater swamps, Global Biogeochemical Cycles, 16, 35-1-35–10, https://doi.org/10.1029/2001GB001594, 2002.

Meijboom, F. and Noordwijk, M. van: Rhizon soil solu-tion samplers as artificial roots, in: Root ecology and its practical application, Verein für Wurzelforschung, A-9020 Klagenfurt Austria, 793–795, 1991.

Morgenstern, A., Overduin, P. P., Günther, F., Stettner, S., Ramage, J., Schirrmeister, L., Grigoriev, M. N., and Grosse, G.: Thermo-erosional valleys in Siberian ice-rich permafrost, Permafrost and Periglacial Processes, 32, 59–75, https://doi.org/10.1002/ppp.2087, 2021.

Morrissey, L. A. and Livingston, G. P.: Methane emissions from Alaska Arctic tundra: An assessment of local spatial variability, 97, 16661–16670, https://doi.org/10.1029/92JD00063, 1992.

Myers-Smith, I. H., Forbes, B. C., Wilmking, M., Hallinger, M., Lantz, T., Blok, D., Tape, K. D., Macias-Fauria, M., Sass-Klaassen, U., Lévesque, E., Boudreau, S., Ropars, P., Hermanutz, L., Trant, A., Collier, L. S., Weijers, S., Rozema, J., Rayback, S. A., Schmidt, N. M., Schaepman-Strub, G., Wipf, S., Rixen, C., Ménard, C. B., Venn, S., Goetz, S., Andreu-Hayles, L., Elmendorf, S., Ravolainen, V., Welker, J., Grogan, P., Epstein, H. E., and Hik, D. S.: Shrub expansion in tundra ecosystems: dynamics, impacts and research priorities, Environ. Res. Lett., 6, 045509, https://doi.org/10.1088/1748-9326/6/4/045509, 2011.

Myhre, G., Samset, B. H., Schulz, M., Balkanski, Y., Bauer, S., Berntsen, T. K., Bian, H., Bellouin, N., Chin, M., Diehl, T., Easter, R. C., Feichter, J., Ghan, S. J., Hauglustaine, D., Iversen, T., Kinne, S., Kirkevåg, A., Lamarque, J. F., Lin, G., Liu, X., Lund, M. T., Luo, G., Ma, X., van Noije, T., Penner, J. E., Rasch, P. J., Ruiz, A., Seland, Ø., Skeie, R. B., Stier, P., Takemura, T., Tsigaridis, K., Wang, P., Wang, Z., Xu, L., Yu, H., Yu, F., Yoon, J. H., Zhang, K., Zhang, H., and Zhou, C.: Radiative forcing of the direct aerosol effect from AeroCom Phase II simulations, 13, 1853–1877, https://doi.org/10.5194/acp-13-1853-2013, 2013.

Neff, J. C. and Hooper, D. U.: Vegetation and climate controls on potential CO2, DOC and DON production in northern latitude soils, 8, 872–884, https://doi.org/10.1046/j.1365-2486.2002.00517.x, 2002.

Neubauer, S. C. and Megonigal, J. P.: Moving Beyond Global Warming Potentials to Quantify the Climatic Role of Ecosystems, Ecosystems, 18, 1000–1013, https://doi.org/10.1007/s10021-015-9879-4, 2015.

Oblogov, G. E., Vasiliev, A. A., Streletskaya, I. D., Zadorozhnaya, N. A., Kuznetsova, A. O., Kanevskiy, M. Z., and Semenov, P. B.: Methane Content and Emission in the Permafrost Landscapes of Western Yamal, Russian Arctic, Geosciences, 10, 412, https://doi.org/10.3390/geosciences10100412, 2020.

Obu, J., Westermann, S., Bartsch, A., Berdnikov, N., Christiansen, H. H., Dashtseren, A., Delaloye, R., Elberling, B., Etzelmüller, B., Kholodov, A., Khomutov, A., Kääb, A., Leibman, M. O., Lewkowicz, A. G., Panda, S. K., Romanovsky, V., Way, R. G., Westergaard-Nielsen, A., Wu, T., Yamkhin, J., and Zou, D.: Northern Hemisphere permafrost map based on TTOP modelling for 2000–2016 at 1 km2 scale, Earth-Science Reviews, 193, 299–316, https://doi.org/10.1016/j.earscirev.2019.04.023, 2019.

Olefeldt, D., Turetsky, M. R., Crill, P. M., and McGuire, A. D.: Environmental and physical controls on northern terrestrial methane emissions across permafrost zones, Global Change Biology, 19, 589–603, https://doi.org/10.1111/gcb.12071, 2013.

Paul, S., Küsel, K., and Alewell, C.: Reduction processes in forest wetlands: Tracking down heterogeneity of source/sink functions with a combination of methods, Soil Biology and Biochemistry, 38, 1028–1039, https://doi.org/10.1016/j.soilbio.2005.09.001, 2006.

Pegoraro, E., Mauritz, M., Bracho, R., Ebert, C., Dijkstra, P., Hungate, B. A., Konstantinidis, K. T., Luo, Y., Schädel, C., Tiedje, J. M., Zhou, J., and Schuur, E. A. G.: Glucose addition increases the magnitude and decreases the age of soil respired carbon in a long-term permafrost incubation study, Soil Biology and Biochemistry, 129, 201–211, https://doi.org/10.1016/j.soilbio.2018.10.009, 2019.

R Core Team: R: A Language and Environment for Statistical Computing, R Foundation for Statistical Computing, Vienna, Austria, 2021.

Rantanen, M., Karpechko, A. Y., Lipponen, A., Nordling, K., Hyvärinen, O., Ruosteenoja, K., Vihma, T., and Laaksonen, A.: The Arctic has warmed nearly four times faster than the globe since 1979, Commun Earth Environ, 3, 1–10, https://doi.org/10.1038/s43247-022-00498-3, 2022.

Robertson, G. P., Coleman, D. C., Sollins, P., and Bledsoe, C. S.: Standard Soil Methods for Long-term Ecological Research, Oxford University Press, 481 pp., 1999.

Roslev, P.Rößger, N., Sachs, T., Wille, C., Boike, J., and King, G. M.: RegulationKutzbach, L.: Seasonal increase of methane oxidationemissions linked to warming in a freshwater wetland by water table changes and anoxia, FEMS Microbiology Ecology, 19, 105–115Siberian tundra, Nat. Clim. Chang., 12, 1031–1036, https://doi.org/10.1111/j.1574-6941.1996.tb00203.x, 19961038/s41558-022-01512-4, 2022.

Schädel, C., Schuur, E. A. G., Bracho, R., Elberling, B., Knoblauch, C., Lee, H., Luo, Y., Shaver, G. R., and Turetsky, M. R.: Circumpolar assessment of permafrost C quality and its vulnerability over time using long-term incubation data, Glob Change Biol, 20, 641–652, https://doi.org/10.1111/gcb.12417, 2014.

Schädel, C., Bader, M. K.-F., Schuur, E. A. G., Biasi, C., Bracho, R., Čapek, P., De Baets, S., Diáková, K., Ernakovich, J., Estop-Aragonés, C., Graham, D. E., Hartley, I. P., Iversen, C. M., Kane, E., Knoblauch, C., Lupascu, M., Martikainen, P. J., Natali, S. M., Norby, R. J., O'Donnell, J. A., Chowdhury, T. R., Šantrůčková, H., Shaver, G., Sloan, V. L., Treat, C. C., Turetsky, M. R., Waldrop, M. P., and Wickland, K. P.: Potential carbon emissions dominated by carbon dioxide from thawed permafrost soils, Nature Clim Change, 6, 950–953, https://doi.org/10.1038/nclimate3054, 2016.

Schädel, C., Beem-Miller, J., Aziz Rad, M., Crow, S. E., Hicks Pries, C. E., Ernakovich, J., Hoyt, A. M., Plante, A., Stoner, S., Treat, C. C., and Sierra, C. A.: Decomposability of soil organic matter over time: the Soil Incubation Database (SIDb, version 1.0) and guidance for incubation procedures, Earth System Science Data, 12, 1511–1524, https://doi.org/10.5194/essd-12-1511-2020, 2020.

Schirrmeister, L., Kunitsky, V., Grosse, G., Wetterich, S., Meyer, H., Schwamborn, G., Babiy, O., Derevyagin, A., and Siegert, C.: Sedimentary characteristics and origin of the Late Pleistocene Ice Complex on north-east Siberian Arctic coastal lowlands and islands – A review, Quaternary International, 241, 3–25, https://doi.org/10.1016/j.quaint.2010.04.004, 2011.

Schirrmeister, L., Froese, D., Tumskoy, V., Grosse, G., and Wetterich, S.: PERMAFROST AND PERIGLACIAL FEATURES | Yedoma: Late Pleistocene Ice-Rich Syngenetic Permafrost of Beringia, in: Encyclopedia of Quaternary Science, Elsevier, 542–552, https://doi.org/10.1016/B978-0-444-53643-3.00106-0, 2013.

Schuur, E. A. G., VogelSchneider, J. G., Crummer, K. G., Lee, H., Sickman, J. O., ., Grosse, G., and Osterkamp, T. E.: The effectWagner, D.: Land cover classification of permafrost thawtundra environments in the Arctic Lena Delta based on old carbon releaseLandsat 7 ETM+ data and net carbon exchange from tundra, 459, 556–559its application for upscaling of methane emissions, Remote Sensing of Environment, 113, 380–391, https://doi.org/10.1038/nature08031016/j.rse.2008.10.013, 2009.

Schuur, E. A. G., Abbott, B. W., Bowden, W. B., Brovkin, V., Camill, P., Canadell, J. G., Chanton, J. P., Chapin, F. S., Christensen, T. R., Ciais, P., Crosby, B. T., Czimczik, C. I., Grosse, G., Harden, J., Hayes, D. J., Hugelius, G., Jastrow, J. D., Jones, J. B., Kleinen, T., Koven, C. D., Krinner, G., Kuhry, P., Lawrence, D. M., McGuire, A. D., Natali, S. M., O'Donnell, J. A., Ping, C. L., Riley, W. J., Rinke, A., Romanovsky, V. E., Sannel, A. B. K., Schädel, C., Schaefer, K., Sky, J., Subin, Z. M., Tarnocai, C., Turetsky, M. R., Waldrop, M. P., Walter Anthony, K. M., Wickland, K. P., Wilson, C. J., and Zimov, S. A.: Expert assessment of vulnerability of permafrost carbon to climate change, Climatic Change, 119, 359–374, https://doi.org/10.1007/s10584-013-0730-7, 2013.

Schuur, E. a. G., McGuire, A. D., Schädel, C., Grosse, G., Harden, J. W., Hayes, D. J., Hugelius, G., Koven, C. D., Kuhry, P., Lawrence, D. M., Natali, S. M., Olefeldt, D., Romanovsky, V. E., Schaefer, K., Turetsky, M. R., Treat, C. C., and Vonk, J. E.: Climate change and the permafrost carbon feedback, Nature, 520, 171–179, https://doi.org/10.1038/nature14338, 2015.

Schwamborn, G., Rachold, V., and Grigoriev, M. N.: Late Quaternary sedimentation history of the Lena Delta, Quaternary International, 89, 119–134, https://doi.org/10.1016/S1040-6182(01)00084-2, 2002.

Serreze, M. C., Walsh, J. E., Chapin, F. S., Osterkamp, T., Dyurgerov, M., Romanovsky, V., Oechel, W. C., Morison, J., Zhang, T., and Barry, R. G.: Observational Evidence of Recent Change in the Northern High-Latitude Environment, Climatic Change, 46, 159–207, https://doi.org/10.1023/A:1005504031923, 2000.

Siewert, M. B., Hugelius, G., Heim, B., and Faucherre, S.: Landscape controls and vertical variability of soil organic carbon storage in permafrost-affected soils of the Lena River Delta, CATENA, 147, 725–741, https://doi.org/10.1016/j.catena.2016.07.048, 2016.

Soil Survey Staff: Keys to Soil Taxonomy, 12th ed., Twelfth Edition, USDA-Natural Resources Conservation Service, Washington, DC, 360 pp., 2014.

Spencer, R. G. M., Mann, P. J., Dittmar, T., Eglinton, T. I., McIntyre, C., Holmes, R. M., Zimov, N., and Stubbins, A.: Detecting the signature of permafrost thaw in Arctic rivers, Geophysical Research Letters, 42, 2830–2835, https://doi.org/10.1002/2015GL063498, 2015.

Strauss, J., Schirrmeister, L., Grosse, G., Wetterich, S., Ulrich, M., Herzschuh, U., and Hubberten, H.-W.: The deep permafrost carbon pool of the Yedoma region in Siberia and Alaska, Geophysical Research Letters, 40, 6165–6170, https://doi.org/10.1002/2013GL058088, 2013a.

Strauss, J., Schirrmeister, L., Grosse, G., Wetterich, S., Ulrich, M., Herzschuh, U., and Hubberten, H.-W.: The deep permafrost carbon pool of the Yedoma region in Siberia and Alaska, Geophysical Research Letters, 40, 6165–6170, https://doi.org/10.1002/2013GL058088, 20132013b.

Symons, G. E. and Buswell, A. M.: The methane fermentation of carbohydrates., vol. 55, J. Am. Chem. Soc., 2028–2036, 1993.

Tabari, H.: Climate change impact on flood and extreme precipitation increases with water availability, Sci Rep, 10, 13768, https://doi.org/10.1038/s41598-020-70816-2, 2020.

Thauer, R. K.: Biochemistry of methanogenesis: a tribute to Marjory Stephenson:1998 Marjory Stephenson Prize Lecture, Microbiology, 144, 2377–2406, https://doi.org/10.1099/00221287-144-9-2377, 1998.

Theisen, A. R. and Murrell, J. C.: Facultative Methanotrophs Revisited, Journal of Bacteriology, 187, 4303–4305, https://doi.org/10.1128/JB.187.13.4303-4305.2005, 2005.

Treat, C. C., Natali, S. M., Ernakovich, J., Iversen, C. M., Lupascu, M., McGuire, A. D., Norby, R. J., Roy Chowdhury, T., Richter, A., Šantrůčková, H., Schädel, C., Schuur, E. A. G., Sloan, V. L., Turetsky, M. R., and Waldrop, M. P.: A pan-Arctic synthesis of CH_4 and CO_2 production from anoxic soil incubations, Glob Change Biol, 21, 2787–2803, https://doi.org/10.1111/gcb.12875, 2015.

Treat, C. C., Marushchak, M. E., Voigt, C., Zhang, Y., Tan, Z., Zhuang, Q., Virtanen, T. A., Räsänen, A., Biasi, C., Hugelius, G., Kaverin, D., Miller, P. A., Stendel, M., Romanovsky, V., Rivkin, F., Martikainen, P. J., and Shurpali, N. J.: Tundra landscape heterogeneity, not interannual variability, controls the decadal regional carbon balance in the Western Russian Arctic, Global Change Biology, 24, 5188–5204, https://doi.org/10.1111/gcb.14421, 2018.

~~Virtanen, T. and Ek, M.: The fragmented nature of tundra landscape, International Journal of Applied Earth Observation and Geoinformation, 27, 4–12, https://doi.org/10.1016/j.jag.2013.05.010, 2014.~~

Turetsky, M. R., Abbott, B. W., Jones, M. C., Walter Anthony, K., Olefeldt, D., Schuur, E. A. G., Koven, C., McGuire, A. D., Grosse, G., Kuhry, P., Hugelius, G., Lawrence, D. M., Gibson, C., and Sannel, A. B. K.: Permafrost collapse is accelerating carbon release, Nature, 569, 32–34, https://doi.org/10.1038/d41586-019-01313-4, 2019.

Wagner, D., Gattinger, A., Embacher, A., Pfeiffer, E.-M., Schloter, M., and Lipski, A.: Methanogenic activity and biomass in Holocene permafrost deposits of the Lena Delta, Siberian Arctic and its implication for the global methane budget, Global Change Biology, 13, 1089–1099, https://doi.org/10.1111/j.1365-2486.2007.01331.x, 2007.

Waldrop, M. P., Wickland, K. P., White Iii, R., Berhe, A. A., Harden, J. W., and Romanovsky, V. E.: Molecular investigations into a globally important carbon pool: permafrost-protected carbon in Alaskan soils, Global Change Biology, 16, 2543–2554, https://doi.org/10.1111/j.1365-2486.2009.02141.x, 2010.

Walz, J., Knoblauch, C., Böhme, L., and Pfeiffer, E.-M.: Regulation of soil organic matter decomposition in permafrost-affected Siberian tundra soils - Impact of oxygen availability, freezing and thawing, temperature, and labile organic matter, Soil Biology and Biochemistry, 110, 34–43, https://doi.org/10.1016/j.soilbio.2017.03.001, 2017.

Walz, J., Knoblauch, C., Tigges, R., Opel, T., Schirrmeister, L., and Pfeiffer, E.-M.: Greenhouse gas production in degrading ice-rich permafrost deposits in northeastern Siberia, Biogeosciences, 15, 5423–5436, https://doi.org/10.5194/bg-15-5423-2018, 2018.

Wang, ~~F. L.~~P., Huang, Q., Tang, Q., Chen, X., Yu, J., Pozdniakov, S. P., and ~~Bettany, J. R.: Influence of Freeze-Thaw~~Wang, T.: Increasing annual and ~~Flooding on the Loss of Soluble Organic Carbon and Carbon Dioxide from Soil, 22, 709–714~~extreme precipitation in permafrost-dominated Siberia during 1959–2018, Journal of Hydrology, 603, 126865, https://doi.org/10.~~2134/jeq1993.00472425002200040011x, 1993~~1016/j.jhydrol.2021.126865, 2021.

Washburn, A. L.: Periglacial processes and environment., St. Martin's Press, New York, 1973.

~~Whiting, G. J. and Chanton, J.~~Westermann, P.: ~~Primary production control~~Temperature regulation of ~~methane emission from~~ methanogenesis in wetlands, ~~364, 794–795~~Chemosphere, 26, 321–328, https://doi.org/10.~~1038/364794a0~~1016/0045-6535(93)90428-8, 1993.

~~Wigley, T. M. L.: The Kyoto Protocol: CO2 CH4 and climate implications, 25, 2285–2288, https://doi.org/10.1029/98GL01855, 1998.~~

~~Yang, S., Liebner, S., Walz, J., Knoblauch, C., Bornemann, T. L. V., Probst, A. J., Wagner, D., Jetten, M. S. M., and in 't Zandt, M. H.: Effects of a long-term anoxic warming scenario on microbial community structure and functional potential of permafrost-affected soil, 32, 641–656, https://doi.org/10.1002/ppp.2131, 2021.~~

Yavitt, J. B., Williams, C. J., and Wieder, R. K.: Production of methane and carbon dioxide in peatland ecosystems across North America: Effects of temperature, aeration, and organic chemistry of peat, Geomicrobiology Journal, 14, 299–316, https://doi.org/10.1080/01490459709378054, 1997.

Yavitt, J. B., Basiliko, N., Turetsky, M. R., and Hay, A. G.: Methanogenesis and Methanogen Diversity in Three Peatland Types of the Discontinuous Permafrost Zone, Boreal Western Continental Canada, Geomicrobiology Journal, 23, 641–651, https://doi.org/10.1080/01490450600964482, 2006.

~~Zimov, S. A., Davydov, S. P., Zimova, G. M., Davydova, A. I., Schuur, E. a. G., Dutta, K., and Chapin, F. S.: Permafrost carbon: Stock and decomposability of a globally significant carbon pool, 33, https://doi.org/10.1029/2006GL027484, 2006.~~

Zhu, X., Wu, T., Li, R., Xie, C., Hu, G., Qin, Y., Wang, W., Hao, J., Yang, S., Ni, J., and Yang, C.: Impacts of Summer Extreme Precipitation Events on the Hydrothermal Dynamics of the Active Layer in the Tanggula Permafrost Region on the Qinghai-Tibetan Plateau, Journal of Geophysical Research: Atmospheres, 122, 11,549-11,567, https://doi.org/10.1002/2017JD026736, 2017.

1175

Formatted: Left, Line spacing: single